JOC The Journal of Organic Chemistry

Article

Redox Active Quinoidal 1,2,4-Benzotriazines

Georgia A. Zissimou, Andreas Kourtellaris, Maria Manoli, and Panayiotis A. Koutentis

J. Org. Chem., **Just Accepted Manuscript** • DOI: 10.1021/acs.joc.8b01311 • Publication Date (Web): 25 Jun 2018

Just Accepted

ACS Publications

is published by the American Chemical Society. 1155 Sixteenth Street N.W., Washington, DC 20036

Redox Active Quinoidal 1,2,4-Benzotriazines

Georgia A. Zissimou, Andreas Kourtellaris, Maria Manoli and Panayiotis A. Koutentis*

Department of Chemistry, University of Cyprus, P.O. Box 20537, 1678 Nicosia, Cyprus

* Corresponding author; e-mail: koutenti@ucy.ac.cy

GRAPHICAL ABSTRACT

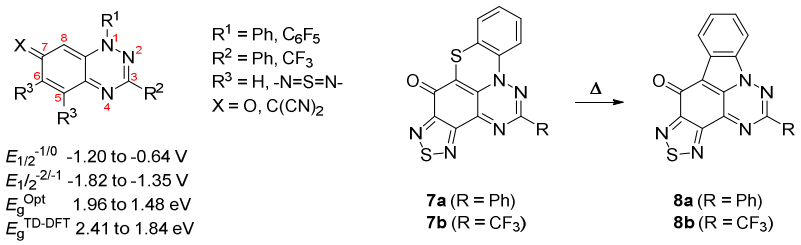

ABSTRACT

Modifying the *para*-quinonimine 1,3-diphenyl-1,2,4-benzotriazin-7(*H*)-one (**2a**) ($E_{1/2}^{-1/0}$ -1.20 V), by replacing the N1-phenyl by pentafluorophenyl, the C3-phenyl by trifluoromethyl, or the C7 carbonyl by ylidenemalononitrile led to improved electron affinities as determined by cyclic voltammetry and computational studies. Combining structural changes further improved electron accepting abilities: the most electron deficient analogues ($E_{1/2}^{-1/0}$ ~-0.65 V) involved combining the ylidene-malononitrile groups at C7 with the trifluoromethyl groups at C3. 1,2,5-Thiadiazolo fusion at C5-C6 did not affect the redox behavior but enhanced the UV-vis absorption profile. During the synthesis of the thiadiazolo analogues, 1,4-thiazino-fused analogues (**6**) were obtained in low yield which thermally ring contract to the triazafluoranthenones (**7**). Compounds are fully characterized, and X-ray data are provided for selected analogues.

1. INTRODUCTION

Redox activity is important in a wide array of biological processes,[1] *e.g.*, cellular respiration[2] and photosynthesis.[3] Furthermore, redox active materials have commercial uses *e.g.*, in metallurgy,[4] as anticorrodants,[5] antioxidants,[6] as components in semiconductors,[7] electrochemical sensors,[8] fuel cells,[9] for radical polymerisations,[10] self-assembled coatings,[11] and many other applications.

Well known redox active organic compounds include acceptors such as fullerene (C_{60}),[12] and tetracyanoquinodimethane (TCNQ),[13] 2,3-dichloro-5,6-dicyano-1,4-benzoquinone (DDQ),[14] as well as donors such as tetrathiafulvalene (TTF),[15] ferrocene,[16] and stable neutral organic radicals (*e.g.*, TEMPO)[17] (Figure 1).

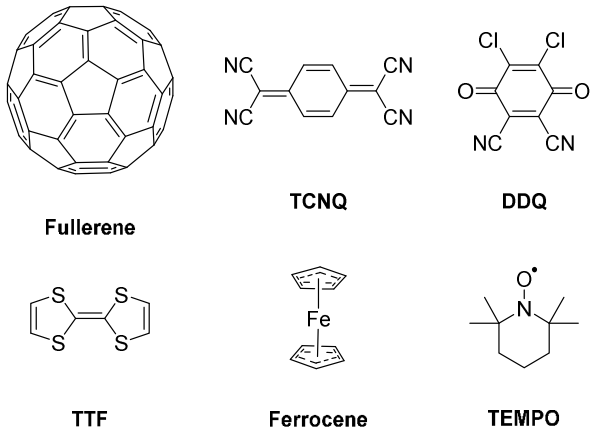

Figure 1. Structures of electron poor (top) and rich (bottom) redox active molecules.

The present interest in organic electronics has led to an increased focus on the synthesis, chemistry, properties and applications of redox active compounds, oligomers and polymers. In particular, the properties of electroactive small organic molecules based on quinoidal motifs have led to their use in electronic applications such as organic photovoltaics,[18] batteries,[19] and spintronic devices.[20]

Considering the above, and as part of our ongoing studies in rare heteroarenes,[21] we began studies on 1,2,4-benzotriazin-4-yls (aka Blatter[22] radicals **1**)[23] which are electron rich but stable neutral organic radicals that have two fully reversible one electron redoxes to give the analogous cation $\mathbf{1}^+$

and anion $\mathbf{1}^-$.[24] Oxidation of radicals **1** affords the analogous benzotriazinones **2**,[25] that can also be prepared by oxidation of *N*-phenylamidrazones **3** (Scheme 1).[23c]

Scheme 1. The Redox Behavior of Benzotriazinyls 1, Preparation and Redox Behavior of Benzotriazinones 2

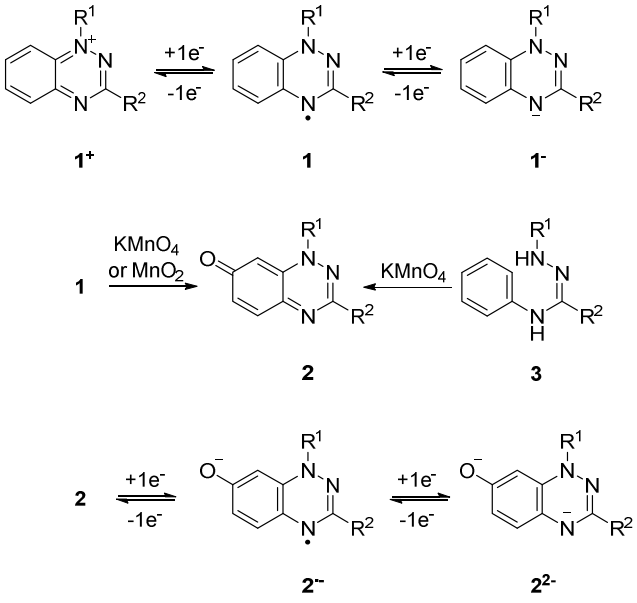

Benzotriazinones are *para*-quinonimines and thus electron deficient redox active species. Electrochemical reduction affords the anion radical ($\mathbf{2}^{\bullet -}$) and dianion ($\mathbf{2}^{2-}$) in succession and both processes are fully reversible (Scheme 1). Benzotriazinones can be readily functionalized with good regioselectivity making them potentially useful building blocks for library synthesis.[26] Furthermore, they can also be used to construct π-extended Blatter radicals,[27] and unusual zwitterionic biscyanines.[28]

Like many other *para*-quinonimines,[29] several 1,2,4-benzotriazinones, show interesting biological properties such as anticancer activity,[30] and as dual inhibitors of β-amyloid (Aβ) fibrillization and acetyl- (AChE) and/or butyryl- (BChE) cholinesterase, all valuable targets for the treatment of Alzheimer's disease.[31] Finally, benzotriazinones have been proposed as potential precursors to stable anion radicals.[32]

Herein, we investigate how structural changes on 1,3-diphenyl-1,2,4-benzotriazin-7(*H*)-one (**2a**, R^1 = R^2 = Ph) affect its electron accepting abilities. Cyclic voltammetry (CV), UV-vis spectroscopy and DFT computational studies were used to investigate the electrochemical window to better understand the redox behavior of these unusual quinoidal benzotriazines.

2. RESULTS AND DISCUSSION

From our in-house compound library, we identified several radicals with suitable electron withdrawing groups (EWGs) at either N1 or C3: the 1-pentafluorophenyl- and 1-(pyrid-2-yl)-substituted 3-phenylbenzotriazinones **1b**[23a] and **1c**[23b] with EWGs at the N1 position, and the 3-trifluoromethyl- and 3-(pyrid-2-yl)- substituted 1-phenylbenzotriazinones **1d**[23b] and **1e**[23b] with EWGs at the C3 position. Radicals **1a-e** were oxidized using MnO_2 (10-50 equiv) to the corresponding quinonimines **2a-e**. Present in our library was also the 1,3-di(pyrid-2-yl)benzotriazinone **2f**[23b] that has EWGs at both N1 and C3, but this was prepared directly from the leuco benzotriazine **1f** (Scheme 2).

Scheme 2. MnO_2-Mediated Oxidation of Benzotriazinyls 1a-f to Benzotriazinones 2a-f

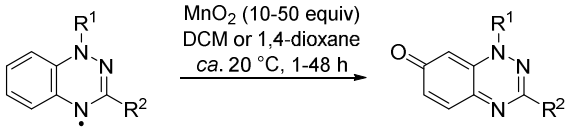

1a (R^1 = R^2 = Ph) **2a** (82%)
1b (R^1 = C_6F_5, R^2 = Ph) **2b** (88%)
1c (R^1 = pyrid-2-yl, R^2 = Ph) **2c** (90%)
1d (R^1 = Ph, R^2 = CF_3) **2d** (93%)
1e (R^1 = Ph, R^2 = pyrid-2-yl) **2e** (46%)
1f (R^1 = R^2 = pyrid-2-yl)[a] **2f** (53%)

[a] **1f** was the leuco form *i.e.* the 1,4-dihydrobenzotriazine

Computational studies (DFT) on the benzotriazinone core [Supporting Information (SI), Section S4] revealed significant molecular orbital density on the N1 positions in both the frontier molecular orbitals (FMOs) but a nodal point exists at the C3 position of the LUMO. This suggested that substitution at N1 and C3 positions will affect the energy of the HOMOs more significantly than that of the LUMOs. Nevertheless, X-ray studies[23a,34] of 1,3-diaryl-1,2,4-benzotriazinyls show that

while the C3-aryl groups are typically in the plane of the benzotriazine, the N1-aryl groups are twisted out of the plane owing to steric interactions with the *peri* C8 hydrogen. As such, substituents at N1 have a predominantly inductive effect, while those on C3 have a combined mesomeric and inductive influence on the electrochemistry of the benzotriazinone scaffold.

CV studies on quinonimines **2a-f** (Table 1) provided useful information to guide the design of more electron poor analogues. The replacement of either the N1 or C3 phenyls (σ_{meta} 0.06, σ_{para} -0.01)[33] by pyrid-2-yl (σ_{meta} 0.33, σ_{para} 0.17)[33] groups led to a similar effect on both redox peaks: the first redox ($E_{1/2}^{-1/0}$) was raised by 0.08 V for the N1 pyridyl **2c** and 0.04 V for the C3 pyridyl **2e**, while the second redox ($E_{1/2}^{-2/-1}$) was raised by 0.14 V and 0.11 V for pyridyl analogues **2c** and **2e**, respectively. These +ve redox shifts showed that substitution at either site moderated the electron affinity of the scaffold (Table 1, entries 3 and 5). Furthermore, while replacing both phenyls by pyridyls (Table 1, entry 6) only led to a 0.08 V +ve shift of the first redox ($E_{1/2}^{-1/0}$) very similar to that seen with the N1 pyridyl **2c**, there was a marked increase in the value of the second redox ($E_{1/2}^{-2/-1}$) which was raised by 0.18 V, *i.e.* combining substitution changes improved the electron affinity of the quinonimine.

CV studies on analogues **2b** and **2d**, with more strongly electron withdrawing pentafluorophenyl (σ_{meta} 0.26, σ_{para} 0.27)[33] and trifluoromethyl (σ_{meta} 0.43, σ_{para} 0.54)[33] groups at N1 and C3, respectively, showed less -ve first redox values **2b** ($E_{1/2}^{-1/0}$ -1.04 V) and **2d** ($E_{1/2}^{-1/0}$ -0.99 V) than the pyridyl analogues **2b,e** and **2f**, but interestingly, their second redox values ($E_{1/2}^{-2/-1}$) were similar (-1.70 and -1.69 V) to the mono pyridyls (-1.68 V and -1.71 V) (Table 1, entries 2, 4-6). Unfortunately, we were unable to prepare the 1,3-di(trifluoromethyl)-, 1,3-di(pentafluorophenyl)-, 1-pentafluorophenyl-3-trifluoromethyl- or 3-pentafluorophenyl-1-trifluoromethyl- substituted benzotriazinones as either the chemistry to make the precursor radicals failed or the required reagents were not available. This prevented our ability to examine combinations of these substituents on the redox behavior. Nevertheless, since the introduction of pentafluorophenyl or

trifluoromethyl groups led to the least -ve redox values, we focused on making further structural changes on quinonimines **2b** and **2d** (Table 1, entries 2 and 4).

Table 1. Optical, Electrochemical and Theoretical Details of 2a-f, 4a-c, 5a,b and 10a,b

entry	compd.	λ_{max}(abs) [nm]	E_g^{Opt} [eV][a]	$E_{1/2}^{-1/0}$ [V]	$E_{1/2}^{-2/-1}$ [V]	$E_g^{TD\text{-}DFT}$ [eV][b]	E_{LUMO} [eV][c]	E_{HOMO} [eV][d]
1	**2a**	639	1.83	-1.20	-1.82	2.25	-3.60	-5.43
2	**2b**	611	1.96	-1.04	-1.70	2.34	-3.76	-5.72
3	**2c**	628	1.86	-1.12	-1.68	2.24	-3.68	-5.54
4	**2d**	626	1.85	-0.99	-1.69	2.41	-3.81	-5.66
5	**2e**	635	1.84	-1.16	-1.71	2.35	-3.64	-5.48
6	**2f**	636	1.85	-1.12	-1.64	2.32	-3.68	-5.53
7	**4a**	780	1.48	-0.85	-1.55	1.95	-3.95	-5.43
8	**4b**	730	1.50	-0.71	-1.46	2.04	-4.09	-5.59
9	**4c**	762	1.58	-0.66	-1.40	2.05	-4.14	-5.72
10	**5a**	645	1.84	-1.10	-1.76	2.16	-3.70	-5.54
11	**5b**	636	1.87	-0.90	-1.69	2.35	-3.90	-5.77
12	**10a**	819	1.49	-0.85	-1.52	1.84	-3.95	-5.44
13	**10b**	810	1.50	-0.64	-1.35	1.96	-4.16	-5.66

[a] E_g^{Opt} was calculated from the onset of the λ_{max} from UV-vis and the Beer-Lambert equation ($E = h*C/\lambda$); [b] $E_g^{TD\text{-}DFT}$ = first excitation energy from TD-DFT/UB3LYP 6-31G(d); [c] $E_{LUMO} = -[E_{1/2}^{-1/0} + 4.8]$ eV; [d] $E_{HOMO} = E_{LUMO} - E_g^{Opt}$ (eV).

UV-vis studies on quinonimines **2a-f** show broad, structured low energy absorption bands between 400 and 700 nm, centered at ~550 nm (Figure 2). Based on TD-DFT calculations (Sect. S4.4, SI) we attributed these low energy bands to transitions between the frontier molecular orbitals (FMOs) (*i.e.* HOMO → LUMO, *f* 0.06-0.09). Varying the substitutents at either N1 or C3, had little effect on the quinonimine's optical band gaps (E_g^{Opt}) which ranged between 1.83-1.96 eV (Table 1). This was owed to the substituent effects being similar in sign and magnitude to both the HOMO and LUMO energy levels (Table S2, SI).

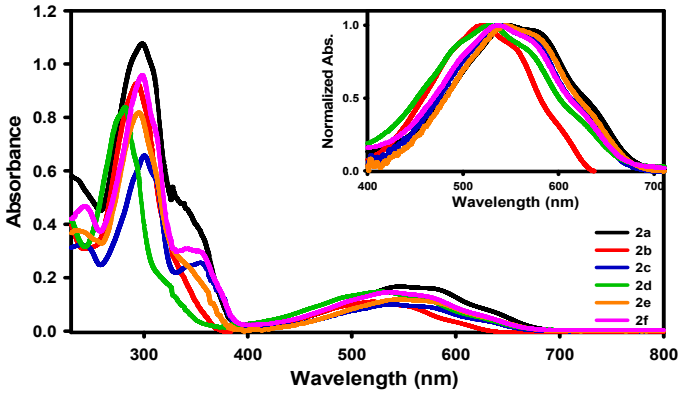

Figure 2. UV-vis of quinonimines **2a** (black), **2b** (red), **2c** (blue), **2d** (green), **2e** (orange) and **2f** (pink) in DCM at ~1.5×10^{-5} mol·L^{-1}.

To increase the electron affinity of quinonimines **2a**,**b** and **2d**, we attempted to convert them into their ylidenemalononitriles **4** (Scheme 3). The ylidenemalononitrile moiety is a powerful electron withdrawing group.[35] This transformation was challenging owing to the strong electron release from the triazine N1 atom to the C7 carbonyl.[26a] Prior studies showed that treating benzotriazinone **2a** with either tetracyanoethylene (TCNE) or tetracyanoethylene oxide (TCNEO) in PhCl heated at *ca.* 140 °C for 18 h afforded the ylidene in low yields (17-19%).[26a] Improved yields were obtained by re-optimizing these reaction conditions: by using TCNEO (1.5 equiv) in anhydrous PhMe, heated at *ca.* 110 °C for only 1 h product **4a** was isolated in 50% yield. These conditions also worked to convert the 1-pentafluorophenyl and 3-trifluoromethyl benzotriazinones **2b** and **2d** into ylidenes **4b** (40%) and **4c** (25%), respectively (Scheme 3).

Scheme 3. Synthesis of Ylidenemalononitriles 4a-c

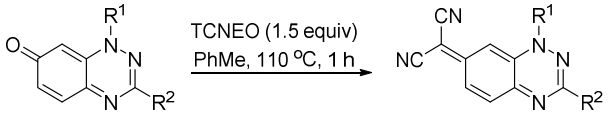

2a ($R^1 = R^2 = Ph$)
2b ($R^1 = C_6F_5$, $R^2 = Ph$)
2d ($R^1 = Ph$, $R^2 = CF_3$)

4a (50%)
4b (40%)
4c (25%)

Ylidenemalononitriles **4a-c** were isolated as blue-green needles that dissolved readily in typical organic solvents. Compared to quinonimines **2** the UV-vis spectra showed substantially red-shifted, broad, structured low energy absorptions between 450-900 nm, centered at ~675 nm (Figure 3). TD-DFT calculations (Sect. S4.4, SI) support that the lowest energy absorptions were owed to transitions between FMOs (*i.e.* HOMO → LUMO, *f* 0.18-0.19) and that the reduction in the optical band gaps (E_g^{Opt} 1.48-1.58 eV) is owed to a lowering of the LUMO energy level relative to the HOMO by ~0.24 eV (Table S2, SI).

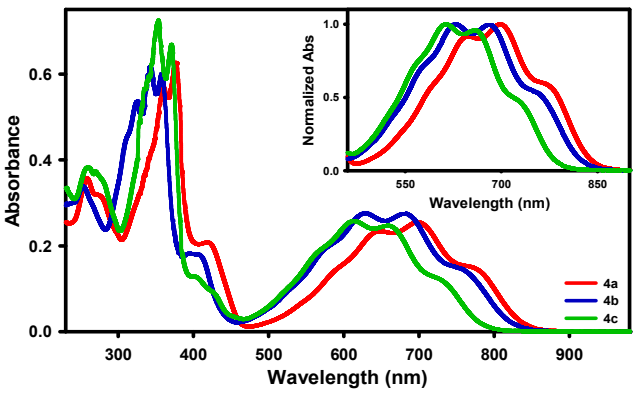

Figure 3. UV-vis of ylidenes **4a** (red), **4b** (blue), and **4c** (green) in DCM at ~1.5×10^{-5} mol·L^{-1}.

Computational DFT studies on ylidenes **4a-c** revealed large dipole moments (μ 5.66-9.23 D) suggesting highly polarized molecules (Sect. S4.3, SI). This was also supported by the ^{13}C NMR data ($CDCl_3$, 500 MHz) that revealed up-field signals of δ_C 65.2 for the ylidenemalononitrile **4a** =*C*$(CN)_2$ resonance that shifted even further up-field to δ_C 58.6 in more polar DMSO-d_6 that can stabilize more readily the polarized resonance form. Typically, the more up-field the signal for the malononitrile C2 signal, the more negative charge, *i.e.* shielding, is associated with that carbon.[36]

CV studies on ylidenes **4a-c** showed that replacing the carbonyl by the ylidenemalononitrile group improved the electron affinities of the molecules (Table 1, entries 7-9). Both the first ($E_{1/2}^{-1/0}$) and second reduction ($E_{1/2}^{-2/-1}$) peaks were +ve shifted by ~0.34 and ~0.27 V, respectively, compared to the analogous quinonimines. Combining the C3 trifluoromethyl and C7 ylidenemalononitrile moieties in compound **4c** gave the analogue with the least negative electron affinity: $E_{1/2}^{-1/0}$ -0.66 V and $E_{1/2}^{-2/-1}$ -1.40 V (Table 1, entry 9).

Additional structural modifications that we investigated included the introduction of 1,2,5-thiadiazole fusion across the C5-C6 benzotriazine bond. 1,2,5-Thiadiazolo-fused arenes are useful electron acceptors in a variety of organic electronic applications (*e.g.*, OPV, OFET, OLED etc).[37] While there are many routes to building benzothiadiazoles,[38] a fast and cheap way to build the ring system directly onto a quinone scaffold is to use tetrasulfur tetranitride (S_4N_4).[39]

Previously, the reaction of benzotriazinone **2a** with S_4N_4 (5 equiv) in DMF at *ca.* 153 °C for 1 h, had given a mixture of the desired thiadiazolo-fused benzotriazinone **5a** (15%) together with a side product, 6-aminobenzotriazinone **6a** (48%).[28] Under these conditions, the reaction of ylidene-malononitriles **4a-c** with S_4N_4 gave only black intractable tars. As such, we prepared the thiadiazolo-fused benzotriazinones **5** first and then converted them into the ylidenemalononitriles **10** (Schemes 4 and 6).

Scheme 4. Preparation of Thiadiazolo-Fused Triazafluoranthenones

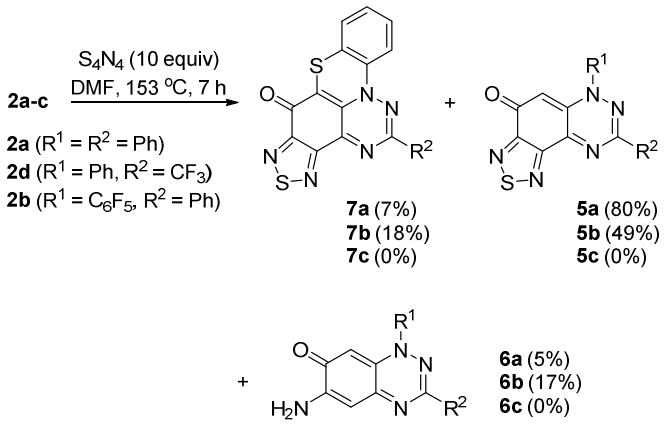

During this effort, we discovered that reacting 6-amino-1,3-diphenylbenzotriazinone **6a** with additional S_4N_4 (5-10 equiv) under the same reaction conditions (DMF, *ca.* 153 °C, 1-12 h), gave the desired thiadiazolobenzotriazinone **5a** in 30% yield. Considering this, we optimized the yield of thiadiazolobenzotriazinone **5a**. Several solvents (1,4-dioxane, PhH, PhMe, PhCl, 1,2-DCB, DMA and DMF) were tested in combinations with different equivalents of S_4N_4 (5-10 equiv), reaction scales and mode of addition. By treating a solution of benzotriazinone **2a** in DMF at *ca*. 153 °C over a 7 h period with five equal portions of S_4N_4 (total 10 equiv) the desired thiadiazolobenzotriazinone **5a** was isolated in high 80% yield, together with a new less polar [R_f 0.78 (*n*-hexane/DCM/*t*-BuOMe, 30:60:10)] red-colored product 2-phenyl-7*H*-[1,2,5]thiadiazolo[3,4-*b*][1,2,4]triazino[1,6,5-*mn*]-phenothiazin-7-one (**7a**) (7%) and a small quantity of 6-amino-1,3-diphenylbenzotriazinone **6a** (5%) (Scheme 4). The use of additional S_4N_4 failed to consume the amino analogue. Using these conditions, the reaction of S_4N_4 with 1-phenyl-

3-(trifluoromethyl)-1,2,4-benzotriazin-7-one **2d** gave a mixture of 2-(trifluoromethyl)-7*H*-[1,2,5]thiadiazolo[3,4-*b*][1,2,4]triazino[1,6,5-*mn*]phenothiazin-7-one (**7b**) (18%), the desired 6-phenyl-8-(trifluoromethyl)-[1,2,5]thiadiazolo[3',4':5,6]benzo[1,2-*e*][1,2,4]-triazin-4(6*H*)-one (**5b**) (49%) and 6-amino-1-phenyl-3-(trifluoromethyl)benzo[*e*][1,2,4]triazin-7(1*H*)-one (**6b**) (17%) (Scheme 4). Unfortunately, the reaction of S_4N_4 with 1-(perfluorophenyl)-3-phenyl-1,2,4-benzotriazinone **2b**, gave a complex reaction mixture (TLC) and no products were isolable in sufficient purity to allow characterization; partly owing to their unstable nature during the work-up.

The structure assignment of the thiazines was supported by elemental analysis, and mass spectrometry which tentatively indicated the additional sulfur. Furthermore, the loss of the benzotriazine H8 resonance in the ^{1}H NMR and the appearance of a splitting pattern for the 1-phenyl suggesting a 1,2-disubstituted arene supported the assignment. Thermolysis of the 1,4-thiazino-fused systems **7a** (R = Ph) and **7b** (R = CF_3) led to the ring contracted triazafluoranthenones **8a** (98%) and **8b** (97%), respectively (Scheme 5). To the best of our knowledge, there is only one report by Rees *et al.*[40] on the thermal ring contraction of 1,4-thiazines. Finally, the thiadiazolo-fused triazafluoranthenone **8a** was also independently prepared in 79% yield by reacting S_4N_4 with triazafluoranthenone **9**,[26b] which helped to further support the structure assignment (Scheme 5).

Scheme 5. Preparation of Thiadiazolo-Fused Triazafluoranthenones 8a and 8b

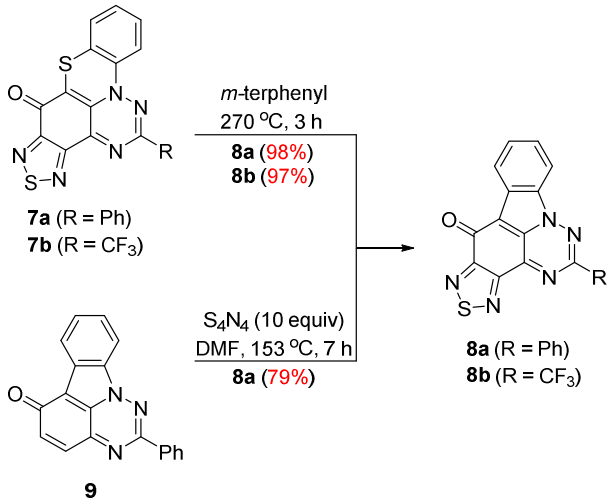

A spectroscopic feature of the 1,4-thiazines was a broad low intensity absorption in the UV-vis spectra that peaked at ~800 nm but extended into the near Infra-Red (NIR), beyond the range of our instrument (Figure 4). TD-DFT calculations (Sect. S4.4, SI) attribute this absorption to a weak HOMO→LUMO transition (f ~0.01) that is accompanied by a redistribution (or charge transfer) of the FMOs from the electron rich benzothiazine to the electron poor thiadiazolobenzotriazine moiety (Figure 5). An Electrostatic Surface Potential (ESP) calculation of thiazine **7a** showed considerable electron deficiency (dark blue) at the thiadiazolobenzotriazinone moiety (Figure 6).

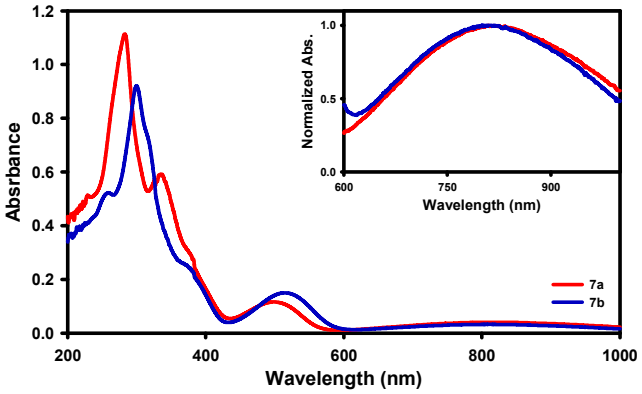

Figure 4. UV-vis of thiazines **7a** (red) and **7b** (blue) in DCM at ~1.5×10^{-5} mol L^{-1}.

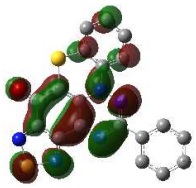

E_{LUMO} = -3.914 eV

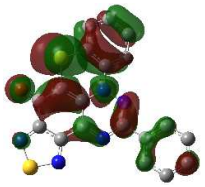

E_{HOMO} = -5.281 eV

Figure 5. FMOs of 2-phenyl-7*H*-[1,2,5]thiadiazolo[3,4-*b*][1,2,4]triazino[1,6,5-*mn*]phenothiazin-7-one (**7a**).

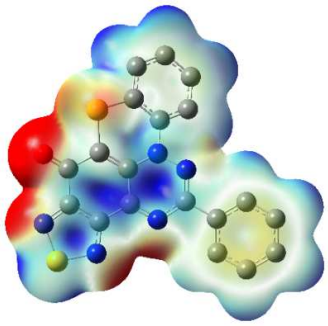

Figure 6. ESP of 2-phenyl-7*H*-[1,2,5]thiadiazolo[3,4-*b*]-[1,2,4]triazino[1,6,5-*mn*]phenothiazin-7-one (**7a**).

Treating the available thiadiazolobenzotriazinones **5a** and **5b** with TCNEO (1.5 equiv.) in PhMe at 110 °C for 1 h gave the desired final thiadiazolo-fused ylidenemalononitriles **10a** (30%) as brown shiny needles, and **10b** (26%) as green metallic plates, respectively.

Scheme 6. Preparation of Thiadiazolo-Fused Triazafluoranthenones 10a and 10b

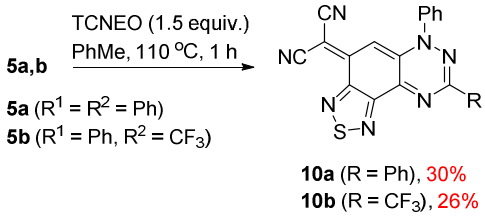

Interestingly, while the 2-phenyl-substituted thiadiazolo ylidenemalononitrile **10a** had a high thermal stability (DSC onset 392.6 °C), the trifluoromethyl **10b** sublimed at *ca*. 280-290 °C (DSC onset 288.2 °C). Comparing the UV-vis data of the thiadiazolo-fused benzotriazines **5a**,**b** (E_g^{Opt} 1.84-1.87 eV) and **10a**,**b** (E_g^{Opt} 1.49-1.50 eV) with their non-thiadiazole-fused analogues **2** (E_g^{Opt} 1.83-1.96 eV) and **4** (E_g^{Opt} 1.48-1.58 eV), respectively showed that thiadiazolo fusion had little effect on the their optical band gaps (Table 1). Nevertheless, all the thiadiazolo-fused benzotriazines showed an additional strong absorption band at around 350-400 nm, leading to broader absorption properties than their non-fused counterparts (Figure 7).

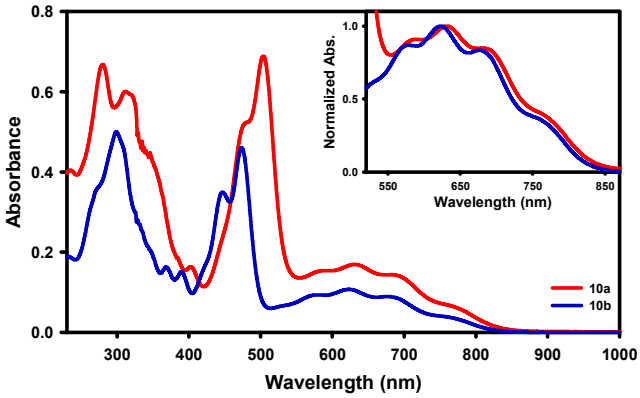

Figure 7. UV-vis of thiadiazolo ylidenemalononitriles **10a** (red) and **10b** (blue) in DCM at ~1.5 × 10^{-5} mol L^{-1}.

CV studies on the thiadiazolo-fused benzotriazinones **5a** (R = Ph) and **5b** (R = CF_3) and (benzotriazinylidene)malononitriles **10a** (R = Ph) and **10b** (R = CF_3) showed that the ring fusion only slightly improved the compounds' electron affinities (Table 1, entries 10-13). For both benzotriazinone **2a** and ylidenemalononitrile **4a**, fusing the 1,2,5-thiadiazole moiety led to a less -ve first reduction potential ($E_{1/2}^{-1/0}$) by ~0.09 V, but only in the case of the benzotriazinone **2a** was the second reduction ($E_{1/2}^{-2/-1}$) affected by a small 0.06 V +ve shift. The improvement in the electron affinity was even less pronounced when the ring fusion was combined with the ylidenemalononitriles **4a** (R = Ph) and **4c** (R = CF_3) with the trifluoromethyl-substituted thiadiazolo-fused ylidene-malononitrile **10b** showing similar reduction potentials to the non-fused ylidenemalononitrile **4c**: ($E_{1/2}^{-1/0}$): **4c** -0.66 V *vs* **10b** -0.64 V and ($E_{1/2}^{-2/-1}$) **4c** -1.40 V *vs* **10b** -1.35 V (Table 1, entries 9 and 13). The data suggested that these structural changes did not have an additive effect on the electrochemistry of the benzotriazine core.

Analysis of the FMOs (Table 1) reveals that the ylidenes **4a-c** (E_{HOMO} -5.72 to -5.29 eV; E_{LUMO} -3.95 to -4.14 eV) and thiadiazolo-fused ylidenes **10a,b** (E_{HOMO} -5.44 to -5.66 eV, E_{LUMO} -3.95 to -4.16 eV), have LUMO energies, comparable to other well-known and widely used electron acceptors, such as fullerene derivatives *e.g.*, [6,6]-phenyl-C71-butyric acid methyl ester (PC70BM, E_{HOMO} -5.90 eV; E_{LUMO} -3.90 eV),[51] and oligothiophene functionalized naphthalene diimides

(E_{HOMO} -6.06 to -5.53 eV; E_{LUMO} -3.97 to -4.14 eV),[52].that are widely used as electron acceptors in OPV devices. The similarity between these FMO energy values tentatively supports that ylidenes **4** and **10** could find use in similar energy applications.

2.1. Crystallography. Single crystal structures of compounds **2b** (CCDC 1840980), **2d** (CCDC 1840989), **4c** (CCDC 1840990) and **10b** (CCDC 1840979) were obtained from bulk recrystallisations enabling a comparison of experimental and computational bond lengths (Table S1, SI). Furthermore, since benzotriazines **2d**, **4c** and **10b** were all N1-phenyl, C3-trifluoromethyl-substituted analogues the data enabled a comparative study of the bond lengths based on the replacement of C=O for $C=C(CN)_2$ and on the effect of thiadiazolo ring fusion on the ylidene.

In general, bond lengths determined *via* computational studies [DFT RB3LYP/6-31G(d)] were similar to those obtained from the X-ray data (σ ~0.01 Å). Bond order analysis supported the quinoidal structure for all analogues with typical carbonyl bond lengths [$d_{(C=O)}$ ~1.23 Å, bond orders ~1.9] (*cf.* cyclohexanone $d_{(C=O)}$ ~1.23 Å).[50] The benzotriazine cores deviated slightly from planarity owing to a very shallow boat conformation for the quinonimine moiety, and the plane angles between the N1-aryl and triazine rings were 52.0–63.7° (X-ray) and 52.6–66.7° (DFT). Interestingly, the ylidenemalononitrile **4c** showed reduced bond orders for the exocyclic [$d_{(C=C)}$ 1.399(3) Å, bond order 1.8] and endocyclic [$d_{(C=C)}$ 1.369(3) Å, bond order 1.9] ethenes separating the N1-phenyl from the ylidenemalononitrile moiety. This suggested a stronger electron release from the triazine N1 to the ylidenemalononitrile, which was expected. Somewhat surprising, was that the thiadiazole fusion moderated this electron release to give marginally longer bond orders for the analogous exocyclic [$d_{(C=C)}$ 1.379(7) Å, bond order 1.9] and endocyclic [$d_{(C=C)}$ 1.379(7) Å, bond order 1.9] ethenes. The thiadiazole bond lengths [$d_{(N-S)}$ ~1.62 Å and $d_{(C=N)}$ ~1.33 Å] were typically aromatic (bond orders ~1.5), suggesting considerable delocalization (*cf.* compound **10b**, Figure 8). Benzotriazinone bond length comparisons between the N1-pentafluorophenyl **2b** and the C3-trifluoromethyl **2d** revealed insignificant differences, nevertheless, the N1-pentafluorophenyl was

significantly more twisted out of the benzotriazinyl plane (66.7°) than the N1-phenyl group of **2d** (52.9°).

ESP calculations for the two best electron acceptors the ylidenemalononitriles **4c** [$E_{1/2}^{-1/0}$ -0.66 V and $E_{1/2}^{-2/-1}$ -1.40 V (Table 1, entry 9)] and **10b** [$E_{1/2}^{-1/0}$ -0.64 V and $E_{1/2}^{-2/-1}$ -1.35 V (Table 1, entry 13)] (Figure 9) show in deep blue color the regions most deficient in electron density, which are predominantly over the triazinyl moiety but extend in the latter case over the thiadiazole.

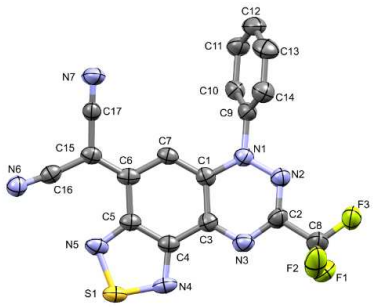

Figure 8. X-ray structure of thiadiazolo-fused benzotriazine **10b**. (CCDC 1840979). Thermal ellipsoids are at 50% probability. Crystallographic number showing. Hydrogens removed for clarity.

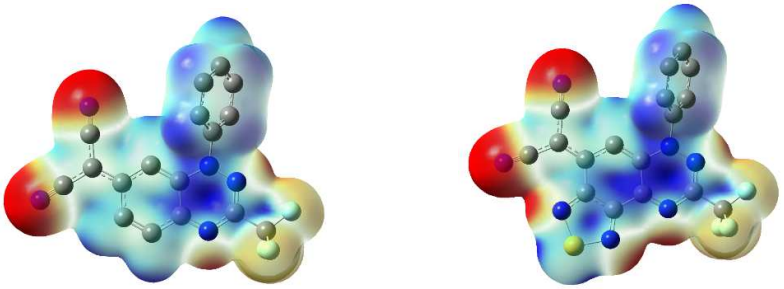

Figure 9. ESP for ylidene **4c** (left) and thiadiazolo-fused benzotriazine **10b** (right).

3. CONCLUSION

Structural modifications on 1,3-diphenyl-1,2,4-benzotriazin-7(*H*)-one (**2a**) ($E_{1/2}^{-1/0}$ -1.20 V) gave compounds with superior electron accepting capabilities. The combination of a C3 trifluoromethyl and C7 ylidenemalononitrile groups gave analogues **4c** and **10b** with significantly reduced first reduction potentials ($E_{1/2}^{-1/0}$ ~-0.65 V). Furthermore, FMO energies for these analogues are similar

in value to known electron acceptors such as PC70BM which suggests that they could act as electron accepting components in electronic devices. The preparation of 1,2,5-thiadiazolo-fused analogues **5a**,**b** using S_4N_4 also led to unusual 1,4-thiazino-fused side-products **7a**,**b** that undergo a rare ring contraction on thermolysis to give triazafluoranthoneone **8a**,**b**. which were independently synthesized. Further studies to understand their chemistry and potential applications are underway.

4. EXPERIMENTAL SECTION

4.1. General Methods and Materials. Dichloromethane (DCM) was dried over CaH_2 and toluene over molecular sieves (4 Å) in a Dean-Stark apparatus prior to use. All volatiles were removed under reduced pressure. All reaction mixtures and column eluents were monitored by TLC using commercial glass backed thin layer chromatography (TLC) plates (Merck Kieselgel 60 F_{254}). The plates were observed under UV light at 254 and 365 nm. The technique of dry flash chromatography was used throughout for all prep scale chromatographic separations using Merck Silica Gel 60 (less than 0.063 mm).[53] Melting and decomposition points were determined using either a PolyTherm-A, Wagner & Munz, Kofler-Hotstage Microscope apparatus or a TA Instruments DSC Q1000. Differential scanning calorimetry (DSC) was used to determine melting and decomposition points with samples hermetically sealed in aluminum pans under an argon atmosphere, using heating rates of 5 °C/min. DSC can often provide thermal decomposition points which appear as exothermic signals. Typically, the pans are opened after seeing an exothermic signal to confirm the material has decomposed rather than a chemical transformation to other isolable product(s). Solvents used for recrystallisation are indicated after the melting point. UV-vis spectra were obtained using a Perkin-Elmer Lambda-25 UV-vis spectrophotometer and inflections are identified by the abbreviation ‘inf”. IR spectra were recorded on a Shimadzu FTIR-NIR Prestige-21 spectrometer with a Pike Miracle Ge ATR accessory and strong, medium and weak peaks are represented by s, m and w, respectively. ^{1}H and ^{13}C (APT) NMR spectra were recorded on either a BrukerAvance 500 machine (at 500 and 125 MHz, respectively) or on a Bruker 300

instrument (at 300 and 75 MHz, respectively). Deuterated solvents were used for homonuclear lock and the signals are referenced to the deuterated solvent peaks. MALDI-TOF MS were conducted on a Bruker BIFLEX III time-of-flight (TOF) mass spectrometer using positive ionization mode. 2,5-Dihydroxybenzoic acid (DHB)[54] and 2B graphite pencil[55] were used as calibrant and/or matrix as indicated. Elemental analysis was performed on a PerkinElmer 2400 series elemental analyzer by Stephen Boyer of London Metropolitan University. Tetrasulfur tetranitride (S_4N_4),[56] tetracyanoethylene oxide (TCNEO),[57] 1-(perfluorophenyl)-3-phenyl-1,4-dihydro-1,2,4-benzotriazin-4-yl (**1b**),[23a] 1,3-diphenyl-1,2,4-benzotriazin-7-one (**2a**),[23c] 3-phenyl-1-(pyrid-2-yl)-1,2,4-benzotriazin-7-one (**2c**),[30a] 1-phenyl-3-(trifluoromethyl)-1,2,4-benzotriazin-7-one (**2d**),[30b] 1-phenyl-3-(pyrid-2-yl)-1,2,4-benzotriazin-7-one (**2e**),[30a] 1,3-di(pyrid-2-yl)-1,2,4-benzotriazin-7-one (**2f**)[23b] and 2-phenyl-6*H*-[1,2,4]triazino[5,6,1-*jk*]carbazol-6-one (**9**)[26b] were prepared according to the literature.

4.2. Cyclic Voltammetry. The concentrations of all studied compounds were 0.001 mol·L^{-1} in dry (over CaH_2) HPLC grade DCM (5 mL) containing *n*-Bu_4NPF_6 (0.1 M) as a supporting electrolyte. A three-electrode electrochemical cell was employed with glassy carbon (3 mm diameter), Pt wire and Ag/AgCl (1 M KCl) as working, counter and reference electrodes, respectively. The ferrocene/ferrocenium (Fc/Fc^+) couple was used as an internal reference and all redox couples are referenced against it ($E_{Fc/Fc+}$ 0.0 V). Scan rate 100 mV·s^{-1}. Temp 20 °C. The calculation of E_{LUMO} was performed according to the simplified empirical equation: $E_{LUMO} = -[E_{1/2}^{-1/0} + 4.8]$ eV, where value "4.8" represents the value of the ferrocene's E_{HOMO} (-4.8 eV *in vacuo*). The HOMO levels were calculated by incorporating the optical band gap according to the following empirical equation: $E_{HOMO} = E_{LUMO} - E_g^{Opt}$.

4.3. X-Ray Crystallography. Data were collected on an Oxford Di□raction Supernova di□ractometer, equipped with a CCD area detector using Mo-Kα radiation (λ = 0.7103 Å) for compound **4c** and Cu-Kα radiation (λ = 1.5418 Å) for compounds **2b**, **2d** and **10b**. A suitable

crystal was attached to glass fibers using paratone-N oil and transferred to a goniostat where they were cooled for data collection. Unit cell dimensions were determined and refined by using 3152 ($4.06 \leq \theta \leq 74.14°$), 1983 ($6.74 \leq \theta \leq 72.24°$), 2189 ($3.06 \leq \theta \leq 28.82°$) and 2992 ($4.72 \leq \theta \leq 66.99°$) reflections for **2b**, **2d**, **4c** and **10b**, respectively. Empirical absorption corrections (multiscan based on symmetry-related measurements) were applied using CrysAlis RED software.[58] The structures were solved by direct method and refined on F^2 using full-matrix least-squares using SHELXL97 or SHELXL2014.[59] Software packages used CrysAlis CCD[58] for data collection, CrysAlis RED[58] for cell refinement and data reduction, WINGX for geometric calculations,[60] and DIAMOND[61] for molecular graphics. The non-H atoms were treated anisotropically. The hydrogen atoms were placed in calculated, ideal positions and refined as riding on their respective carbon atoms.

Crystal refinement data for compound **2b** (CCDC 1840980): $C_{19}H_8F_5N_3O$, M = 389.28, monoclinic, space group $P2_{1/n}$, a = 12.1586(7) Å, b = 6.2942(4) Å, c = 20.7512(12) Å, α = 90°, β = 95.028(5)°, γ = 90°, V = 1581.95(16) Å^3, Z = 4, T = 100(2) K, ρ_{calcd} = 1.634 g cm^{-3}, $2\theta_{max}$ = 67. Refinement of 253 parameters on 2086 independent reflections out of 3152 measured reflections (R_{int} = 0.0294) led to R_1 = 0.0585 [I > 2σ(I)], wR_2 = 0.2158 (all data), and S = 1.081with the largest difference peak and hole of 0.369 and -0.414 e^{-3}, respectively.

Crystal refinement data for compound **2d** (CCDC 1840989): $C_{14}H_8F_3N_3O$, M = 291.23, orthorhombic, space group $P\ b\ c\ a$, a = 15.4804(4) Å, b = 7.6884(2) Å, c = 20.7339(6) Å, $\alpha = \beta = \gamma$ = 90°, V = 2467.74(12) Å^3, Z = 8, T = 100(2) K, ρ_{calcd} = 1.568 g cm^{-3}, $2\theta_{max}$ = 67. Refinement of 190 parameters on 2198 independent reflections out of 15140 measured reflections (R_{int} = 0.0340) led to R_1 = 0.0366 [I > 2σ(I)], wR_2 = 0.1035 (all data), and S = 1.106 with the largest difference peak and hole of 0.244 and -0.280 e^{-3}, respectively.

Crystal refinement data for compound **4c** (CCDC 1840990): $C_{17}H_8F_3N_5$, M = 339.22, triclinic, space group P -1, a = 6.7763(9) Å, b = 8.5591(7) Å, c = 13.2125(14) Å, α = 95.469(8)°, β =

100.076(10)°, γ = 99.918(9)°, V = 736.98(14) Å^3, Z = 2, T = 100(2) K, ρ_{calcd} = 1.671 g cm^{-3}, $2\theta_{max}$ = 25. Refinement of 226 parameters on 2585 independent reflections out of 4562 measured reflections (R_{int} = 0.0305) led to R_1 = 0.0485 [I > 2σ(I)], wR_2 = 0.1291 (all data), and S = 1.006 with the largest difference peak and hole of 0.611 and -0.497 e^{-3}, respectively.

Crystal refinement data for compound **10b** (CCDC 1840979): $C_{17}H_6F_3N_7S$, M = 397.35, monoclinic, space group $P2_{1/c}$, a = 9.7769(7) Å, b = 27.140(3) Å, c = 6.6499(7) Å, α = 90°, β = 106.914(9)°, γ = 90°, V = 1688.2(3) Å^3, Z = 4, T = 100(2) K, ρ_{calcd} = 1.563 g cm^{-3}, $2\theta_{max}$ = 67. Refinement of 253 parameters on 2992 independent reflections out of 5880 measured reflections (R_{int} = 0.0607) led to R_1 = 0.0715 [I > 2σ(I)], wR_2 = 0.2159 (all data), and S = 0.940 with the largest difference peak and hole of 0.541 and -0.644 e^{-3}, respectively.

4.4. Computational Methods. Restricted polarized density functional theory (RDFT) utilizing the hybrid B3LYP method was used for all calculations employing the 6-31G(d) basis set to calculate all properties.[62] The geometries of the close shell singlet were fully optimized, and analytical second derivatives were computed using vibrational analysis to confirm each stationary point to be a minimum by yielding zero imaginary frequencies. All the energies were corrected after zero-point energies (ZPE) were scaled by 0.981 according to the equation: $^{GS}E_{TOT} = E_{GS} + (ZPE \times SF)$.[63] TD-DFT calculations were performed at the RB3LYP/6-31G(d) level of theory to calculate the vertical excitation energy. The latter in combination with the HOMO energy taken from the optimization calculations provide a more accurate energy for the LUMO orbital according to the equation: $E_{LUMO} = E_{HOMO} + E_{HOMO \rightarrow LUMO}$. All the above computations were performed using the Gaussian 03 suite of programs.[64]

4.5. Synthesis of 1-(Perfluorophenyl)-3-phenyl-1,2,4-benzotriazin-7-one (2b). To a vigorously stirred solution of 1-(perfluorophenyl)-3-phenyl-1,4-dihydro-1,2,4-benzotriazin-4-yl (**1b**) (374.3 mg, 1.0 mmol) in dry DCM (10.0 mL) at *ca*. 20 °C was added MnO_2 (869.4 mg, 10.0 mmol). After 1 h the radical X was fully consumed (by TLC) and the reaction was judged complete. The mixture

was then filtered through Celite®, that was then rinsed with DCM (50 mL). The filtrate and DCM washings were combined, and the volatiles removed *in vacuo*. Chromatography (*n*-hexane/*t*-BuOMe, 50:50) of the residue afforded the *title compound* **2b** (342.6 mg, 88%) as dark purple cubes; mp (hot-stage) decomp.: 218.9–220.1 °C (PhMe); mp (DSC) decomp. onset: 208.6 °C, decomp. peak max: 215.3 °C (PhMe); R_f 0.58 (*n*-hexane/*t*-BuOMe, 50:50); Anal. Calcd for $C_{19}H_8F_5N_3O$: C, 58.62; H, 2.07; N, 10.79. Found: C, 58.83; H, 2.11; N, 10.85%; λ_{max}(DCM)/nm 278 inf (log ε 4.47), 293 (4.56), 305 inf (4.47), 340 inf (3.86), 485 inf (3.54), 520 (3.63), 562 inf (3.52), 611 inf (2.94); ν_{max}/cm^{-1} 1624m, 1611m, 1555m, 1518s, 1460m, 1443m, 1327m, 1244m, 1105m, 1069m, 1009m, 991s, 918s, 866m, 785m, 766m, 725m, 700s; δ_H(500 MHz, $CDCl_3$) 8.21–8.19 (2H, m), 7.70 (1H, d, *J* 10.0, *H*-5), 7.52–7.48 (3H, m), 7.25 (1H, dd, *J* 10.0, 2.0, *H*-6, overlap with $CDCl_3$), 5.66 (1H, d, *J* 1.5, *H*-8); δ_C(125 MHz, $CDCl_3$) one C (s) resonance missing, 182.5 (s, *C*-8), 156.3 (s), 151.3 (s), 143.5 (dm, $^1J_{CF}$ 270.0), 143.1 (dm, $^1J_{CF}$ 258.8), 142.2 (d), 138.4 (dm, $^1J_{CF}$ 246.3) 135.7 (s), 133.0 (d), 131.1 (d), 128.9 (d), 126.8 (d), 115.1 (s), 97.6 (d); *m/z* (MALDI-TOF) 390 (MH^+, 47%), 389 (M^+, 5), 374 (27), 242 (100).

4.6. Synthesis of Benzo-1,2,4-triazin-7-ylidenemalononitriles 4a-c.

*4.6.1. 2-(1,3-Diphenylbenzo[e][1,2,4]triazin-7(1*H*)-ylidene)malononitrile (**4a**)*. To a stirred solution of 1,3-diphenyl-1,2,4-benzotriazin-7-one (**2a**) (60.0 mg, 0.2 mmol) in toluene (2 mL) at *ca.* 20 °C was added TCNEO (43.3 mg, 0.3 mmol) and the reaction mixture was then immersed into a pre-heated (~115 °C) oil bath. The reaction mixture was heated at reflux for 1 h, cooled to *ca*. 20 °C, poured over a silica dry flash column and chromatographed (DCM) to afford the *title compound* **2a** (34.8 mg, 50%) as blue needles; mp (hot-stage) not observed; mp (DSC) onset: 320.0 °C, peak max: 320.3 °C (PhMe) (lit.[26a] 306–311 °C); R_f 0.48 (DCM); λ_{max}(DCM)/nm 258 (log ε 4.45), 277 inf (4.40), 337 (4.47), 359 (4.65), 376 inf (4.69), 418 (4.22), 586 inf (4.05), 644 (4.26), 698 (4.30), 780 (4.05); ν_{max}/cm^{-1} 3061w (aryl C-H), 2203s (C≡N), 1612m, 1551m, 1508s, 1489s, 1377s, 1364m, 1341m, 1306s, 1267s, 1188m, 1152m, 1136m, 1003m, 841s, 833m, 781m, 752s; δ_H(500 MHz,

$CDCl_3$) 8.26 (2H, d, *J* 6.5), 7.94 (1H, dd, *J* 9.5, 1.5, *H*-6), 7.70–7.59 (6H, m), 7.52–7.46 (3H, m), 6.59 (1H, d, *J* 1.5, *H*-8); δ_H(500 MHz, 80 °C, DMSO-d_6) 8.24–8.22 (2H, m), 7.92 (1H, d, *J* 9.5), 7.85–7.81 (3H, m), 7.78–7.71 (3H, m), 7.58–7.57 (3H, m), 6.32 (1H, d, *J* 1.0, *H*-8); δ_C(125 MHz, 80 °C, DMSO-d_6) 155.2 (s), 153.0 (s), 152.1 (s), 140.2 (s), 136.5 (d), 135.4 (s), 132.9 (d), 130.6 (d), 130.5 (d), 130.3 (d), 129.7 (d), 128.5 (d), 126.3 (d), 125.3 (s), 115.9 (s, *C*≡N), 115.8 (s, *C*≡N), 93.8 (d), 58.6 [s, $C(CN)_2$]; *m/z* (MALDI-TOF) 348 (MH^+, 21%), 347 (M^+, 100); identical to an authentic sample.

*4.6.2. 2-[1-(Perfluorophenyl)-3-phenylbenzo[*e*][1,2,4]triazin-7(1*H*)-ylidene]malononitrile (**4b**).* To a stirred solution of 1-(perfluorophenyl)-3-phenylbenzo[*e*][1,2,4]triazin-7(1*H*)-one (**2b**) (77.8 mg, 0.2 mmol) in toluene (2 mL) at *ca.* 20 °C was added TCNEO (43.3 mg, 0.3 mmol) and the reaction mixture was then immersed in a pre-heated (~115 °C) oil bath. The reaction mixture was heated at reflux for 1 h, cooled to *ca*. 20 °C, poured over a silica flash column and chromatographed (DCM) to afford the *title compound* **4b** (35.0 mg, 40%) as blue needles; mp (hot-stage) 277.0–278.1 °C (PhMe); mp (DSC) onset: 275.4 °C, peak max: 278.8 °C (PhMe); R_f 0.75 (DCM); Anal. Calcd for $C_{22}H_8F_5N_5 \cdot 1.5$ PhMe: C, 67.82; H, 3.50; N, 12.17. Found: C, 67.80; H, 3.37; N, 11.87%; λ_{max}(DCM)/nm 259 (log ε 4.54), 280 inf (4.50), 334 inf (4.71), 353 (4.82), 370 (4.78), 402 inf (4.07), 427 inf (3.91), 515 inf (3.89), 563 inf (4.22), 612 (4.37), 661 (4.35), 730 inf (4.04); ν_{max}/cm^{-1} 2207s (C≡N), 1514s, 1389m, 1385m, 1337m, 1331m, 1302m, 1277m, 1179m, 1148m, 1123m, 1074m, 1015m, 995s, 920s, 837s, 785m, 760m, 735m, 721m; δ_H(500 MHz, $CDCl_3$) 8.18 (2H, dd, *J* 7.0, 2.0), 7.93 (1H, dd, *J* 9.5, 2.0, *H*-6), 7.57 (1H, d, *J* 9.5, *H*-5), 7.55-7.48 (3H, m), 7.27–7.24 (2.6H, m, overlap with $CDCl_3$, PhMe), 7.18–7.14 (1.8H, m, PhMe), 6.09 (1H, d, *J* 1.5, *H*-8), 2.36 (1.8H, PhMe); δ_C(125 MHz, $CDCl_3$) one C (s) and one *C*F resonance missing, 157.3 (s), 154.2 (s), 152.9 (s), 143.5 (dm, $^1J_{CF}$ 254.4), 137.9 (s, PhMe), 138.6 (dm, $^1J_{CF}$ 215.8), 137.8 (d), 133.9 (s), 132.4 (s), 131.7 (d), 131.2 (d), 129.0 (d, PhMe), 129.0 (d), 128.2 (d, PhMe), 127.1 (d), 125.3 (d, PhMe), 114.8 (s, *C*≡N), 114.4 (s, *C*≡N), 90.3 (d), 70.4 [s, $C(CN)_2$], 21.4 (t, PhMe); *m/z* (MALDI-TOF) 438 (MH^+, 17%), 437 (M^+, 100).

*4.6.3. 2-[1-Phenyl-3-(trifluoromethyl)benzo[*e*][1,2,4]-triazin-7(1*H*)-ylidene]malononitrile (**4c**).* To a stirred solution of 1-phenyl-3-(trifluoromethyl)benzo[*e*][1,2,4]triazin-7(1*H*)-one (**2d**) (58.3 mg, 0.2 mmol) in toluene (2 mL) at *ca.* 20 °C was added TCNEO (43.3 mg, 0.3 mmol) and the reaction mixture was then immersed into a pre-heated (~115 °C) oil bath. The reaction mixture was heated at reflux for 1 h, cooled to *ca*. 20 °C, poured over a silica flash column and chromatographed (DCM) to afford the *title compound* **4c** (17.0 mg, 25%) as green-blue needles; mp (hot-stage) 242.2–245.3 °C (*n*-hexane); mp (DSC) onset: 245.8 °C, peak max: 247.1 °C (*n*-hexane); R_f 0.65 (DCM); Anal. Calcd for $C_{17}H_8F_3N_5$: C, 60.18; H, 2.38; N, 20.64. Found: C, 60.15; H, 2.28; N, 20.51%; λ_{max}(DCM)/nm 253 (log ε 4.12), 309 inf (4.23), 325 (4.32), 342 (4.38), 358 (4.37), 401 (3.84), 569 inf (3.85), 627 (4.03), 682 (4.02), 762 inf (3.73); ν_{max}/cm^{-1} 3103w and 3057w (aryl C-H), 2203m (C≡N), 1555m, 1530s, 1493s, 1416s, 1371s, 1352s, 1233s, 1206m, 1190s, 1167s, 1152s, 1134s, 1105s, 995s, 893m, 845s, 829m, 799m, 762s, 716s; δ_H(500 MHz, $CDCl_3$) 7.95 (1H, dd, *J* 9.5, 1.0, *H*-6), 7.69–7.62 (3H, m), 7.55–7.51 (3H, m), 6.56 (1H, d, *J* 1.5, *H*-8); δ_C(125 MHz, $CDCl_3$) 157.9 (s), 153.2 (s), 145.5 (q, $^2J_{CF}$ 38.8, *C*CF_3), 139.2 (s), 138.7 (d), 134.7 (s), 131.4 (d), 130.7 (d), 130.4 (d), 124.8 (d), 118.8 (q, $^1J_{CF}$ 272.5, *C*F_3), 114.4 (s, *C*≡N), 114.3 (s, *C*≡N), 96.4 (d), 70.2 [s, *C*$(CN)_2$]; *m/z* (MALDI-TOF, pencil matrix) 340 (MH^+, 14%), 339 (M^+, 100), 301 (11), 242 (19), 128 (95).

4.7. Synthesis of [1,2,5]Thiadiazolobenzo[1,2,4]triazin-7-ones 5a-b, [1,2,5]Thiadiazolobenzo[1,2,4]triazino[1,6,5]phenothiazin-7-ones 7a-b and 6-Aminobenzo[1,2,4]triazin-7-ones 6a-b.

*4.7.1. 6,8-Diphenyl[1,2,5]thiadiazolo[3',4':5,6]benzo[1,2-*e*][1,2,4]triazin-4(6*H*)-one (**5a**).* To a stirred solution of 1,3-diphenyl-1,2,4-benzotriazin-7-one (**2a**) (60.0 mg, 0.2 mmol) in DMF (4 mL) at *ca*. 20 °C was added S_4N_4 (73.7 mg, 0.4 mmol) and the reaction mixture was heated at *ca*. 153 °C. Over a 5 h period at *ca*. 153 °C, to the reaction mixture was added an additional four portions of S_4N_4 (4 × 73.7 mg). The reaction mixture was heated for a total of 7 h, allowed to cool to *ca*. 20 °C

and then extracted with 50:50 H_2O/DCM (100 mL). The organic layer was separated, washed with additional H_2O (20 mL), dried ($MgSO_4$), filtered and the volatiles were removed in vacuo. Chromatography (DCM/Et_2O, 95:5) gave 2-phenyl-7*H*-[1,2,5]thiadiazolo[3,4-*b*][1,2,4]triazino-[1,6,5-*mn*]phenothiazin-7-one (**7a**) (5.4 mg, 7%) as pink needles; mp (hot-stage) not observed; mp (DSC) onset: 327.2 °C, peak max: 327.4 °C; decomp. onset: 328.0 °C, decomp. peak max: 329.6 °C (PhMe); R_f 0.78 (*n*-hexane/DCM/*t*-BuOMe, 30:60:10); Anal. Calcd for $C_{19}H_9N_5OS_2$: C, 58.90; H, 2.34; N, 18.08. Found: C, 58.95; H, 2.26; N, 18.18%; λ_{max}(DCM)/nm 257 inf (log ε 4.30), 301 (4.55), 320 inf (4.42), 375 inf (3.98), 515 (3.76), 812 (3.10); ν_{max}/cm^{-1} 3067w (aryl C-H), 1609s (C=O), 1582s, 1566s, 1518s, 1497m, 1472m, 1458s, 1433s, 1404s, 1368m, 1348m, 1331s, 1317m, 1275m, 1236s, 1165s, 1121m, 1109m, 945m, 883s, 829s, 777m, 760s, 733s; δ_H(500 MHz, TFA-*d*) 9.09 (1H, d, *J* 8.5), 8.58 (2H, d, *J* 7.5), 8.37 (1H, d, *J* 7.5), 8.13 (1H, dd, *J* 7.8, 7.8), 7.99 (1H, dd, *J* 7.8, 7.8), 7.63–7.58 (3H, m); δ_C(125 MHz, TFA-*d*) 175.7 (s), 159.1 (s), 157.6 (s), 155.6 (s), 152.0 (s), 138.2 (d), 137.7 (s), 135.8 (d), 135.4 (d), 135.3 (d), 134.7 (s), 133.7 (s), 131.7 (d), 130.5 (d), 126.0 (s), 123.7 (d), 106.7 (s); *m/z* (MALDI-TOF) 388 (MH^+, 100%), 387 (M^+, 30), 373 (14), 372 (23), 371 (100). Further elution (DCM/Et_2O, 80:20) afforded *the title compound* **5a** (57.4 mg, 80%) as brown needles; mp (hot-stage) not observed; mp (DSC) onset: 313.6 °C, peak max: 314.9 °C (PhCl) (lit.[28] 285-290 °C); R_f 0.34 (DCM/*t*-BuOMe, 90:10); λ_{max}(DCM)/nm 269 (log ε 4.01), 309 (4.18), 406 (3.75), 499 inf (2.98), 540 (3.09), 580 (3.04), 636 inf (2.73); ν_{max}/cm^{-1} 3067w (aryl C-H), 1612s, 1601s, 1591s, 1574m, 1516s, 1499s, 1466m, 1458m, 1441m, 1406m, 1350m, 1279m, 1236s, 1159m, 1119m, 905m, 831m, 783m, 773s, 746m, 723m; δ_H(500 MHz, $CDCl_3$) 8.39–8.37 (2H, m), 7.69–7.60 (5H, m), 7.55–7.51 (3H, m), 6.26 (1H, s, *H*-8); identical to an authentic sample. Further elution (DCM/Et_2O, 50:50) afforded 6-amino-1,3-diphenyl-1,2,4-benzotriazin-7-one (**6a**) as yellow needles; mp (hot-stage) 279–281 °C (PhH), (lit.[26a] 279–282 °C); R_f 0.21 (*t*-BuOMe/*n*-hexane, 75:25); δ_H (500 MHz; TFA-*d*) NH peak missing, 8.09 (2H, d, *J* 7.6), 7.79–7.65 (7H, m), 7.58–7.48 (3H, m); *m/z* (MALDI-TOF) 316 (MH^++1, 34%), 315 (MH^+, 100), 314 (M^+, 4); identical to an authentic sample.

4.7.2. 6-Phenyl-8-(trifluoromethyl)[1,2,5]thiadiazolo[3',4':5,6]benzo[1,2-e][1,2,4]triazin-4(6H)-one (**5b**). To a stirred solution of 1-phenyl-3-(trifluoromethyl)-1,2,4-benzotriazin-7-one (**2d**) (58.3 mg, 0.2 mmol) in DMF (4 mL) at *ca*. 20 °C was added S_4N_4 (73.7 mg, 0.4 mmol) and the reaction mixture was the heated to *ca*. 153 °C. Over a 5 h period at *ca*. 153 °C, to the reaction mixture was added an additional four portions of S_4N_4 (4 × 73.7 mg). The reaction mixture was heated for a total of 7 h, allowed to cool to *ca*. 20 °C and then extracted with 50:50 H_2O/DCM (100 mL). The organic layer was separated, washed with additional H_2O (20 mL), dried ($MgSO_4$), filtered and the volatiles were removed in vacuo. Chromatography (DCM/Et_2O, 95:5) gave 2-(trifluoromethyl)-7*H*-[1,2,5]thiadiazolo[3,4-*b*][1,2,4]triazino[1,6,5-*mn*]phenothiazin-7-one (**7b**) (13.7 mg, 18%) as red needles; mp (hot-stage) not observed; mp (DSC) onset: 309.7 °C, peak max: 310.8 °C (PhH); R_f 0.83 (*n*-hexane/DCM/*t*-BuOMe, 30:60:10), R_f 0.30 (*n*-hexane/DCM/*t*-BuOMe, 60:30:10); Anal. Calcd for $C_{14}H_4F_3N_5OS_2$: C, 44.33; H, 1.06; N, 18.46. Found: C, 44.46; H, 0.62; N, 18.82%; λ_{max}(DCM)/nm 282 (log ε 4.62), 336 (4.35), 500 (3.64), 819 (3.18); ν_{max}/cm^{-1} 3055w (aryl C-H), 1613s (C=O), 1586s, 1533s, 1491m, 1468s, 1412m, 1385s, 1375m, 1354m, 1335m, 1302m, 1206s, 1153s, 1142s, 1125s, 1115s, 1078m, 1043m, 1038m, 949m, 891s, 868m, 839m, 776s, 768s, 748m, 735s, 718s; δ_H(500 MHz, TFA-*d*) 8.24 (1H, d, *J* 9.0), 7.48 (1H, dd, *J* 6.8, 6.8), 7.36 (1H, br s), 7.16 (1H, d, *J* 7.5); *m/z* (MALDI-TOF, DHB matrix) 380 (MH^+, 21%), 379 (M^+, 100). Further elution (DCM/*t*-BuOMe, 80:20) afforded the *title compound* **5b** (34.3 mg, 49%) as purple needles; mp (hot-stage) 230.2–232.2 °C (PhH); mp (DSC) onset: 235.1 °C, peak max: 236.0 °C (PhH); R_f 0.64 (DCM/*t*-BuOMe, 90:10); Anal. Calcd for $C_{14}H_6F_3N_5OS$: C, 48.14; H, 1.73; N, 20.05. Found: C, 48.27; H, 1.75; N, 20.04%; λ_{max}(DCM)/nm 259 (log ε 4.35), 298 (4.33), 311 (4.32), 324 (4.21), 372 (3.82), 390 (3.77), 457 inf (3.22), 492 inf (3.39), 526 (3.45), 571 inf (3.33), 624 inf (2.91); ν_{max}/cm^{-1} 3061w (aryl C-H), 1626s, 1586m, 1547s, 1491m, 1396s, 1350m, 1240s, 1206s, 1138s, 1115m, 1103s, 1049s, 908s, 858m, 839m, 829s, 791m, 773s; δ_H(500 MHz, $CDCl_3$) 7.68–7.61 (3H, m), 7.54–7.53 (2H, m), 6.19 (1H, s, *H*-8); δ_C(125 MHz, $CDCl_3$) 173.6 (s, C=O), 157.3 (s), 151.9 (s), 151.3 (s), 142.4 (q, $^2J_{CF}$ 38.8), 140.1 (s), 139.7 (s), 131.1 (d), 130.7 (d), 125.1 (d), 119.0 (q, $^1J_{CF}$

272.5), 100.6 (d); *m/z* (MALDI-TOF) 350 (MH^+, 100%). Further elution (DCM/Et_2O, 50:50) gave 6-amino-1-phenyl-3-(trifluoromethyl)-1,2,4-benzotriazin-7-one (**6b**) (10.5 mg, 17%) as orange needles; mp (hot-stage) not observed (PhH); mp (DSC) onset: 349.4 °C, peak max: 352.1 °C (PhH); R_f 0.65 (DCM/*t*-BuOMe, 50:50); Anal. Calcd for $C_{14}H_9F_3N_4O$: C, 54.91; H, 2.96; N, 18.29. Found: C, 54.84; H, 2.92; N, 18.38%; λ_{max}(DCM)/nm 266 (log ε 3.97), 284 inf (3.81), 323 inf (3.18), 374 inf (3.19), 396 inf (3.56), 416 (3.66), 495 inf (2.68); ν_{max}/cm^{-1} 3381w, 3300w, 3233m and 3196m (N-H), 1578s, 1574s, 1551s, 1505m, 1493m, 1416m, 1393m, 1285s, 1198s, 1155s, 1130s, 1092m, 1063m, 995s, 855m, 830m, 772s, 756m; δ_H(500 MHz, DMSO-d_6) 8.62 (1H, br s, N*H*), 7.80 (1H, br s, NH), 7.70–7.64 (5H, m), 6.73 (1H, s, *H*-8), 5.64 (1H, s, *H*-5); δ_C(125 MHz, DMSO-d_6) 173.2 (s, C=O), 155.3 (s), 151.7 (s), 142.6 (q, $^2J_{CF}$ 35.0), 140.8 (s), 136.3 (s), 130.2 (d), 129.9 (d), 126.1 (d), 119.8 (q, $^1J_{CF}$ 272.5), 98.0 (d), 95.0 (d); *m/z* (MALDI-TOF) 308 (MH^++1, 9%), 307 (MH^+, 100).

4.8. Synthesis of 1,2,5-Thiadiazolo-1,2,4-triazino-1,6,5-carbazol-7-ones (Triazafluoranthenones) 8a-b.

*4.8.1. 2-Phenyl-7*H*-[1,2,5]thiadiazolo[3,4-*b*][1,2,4]triazino[1,6,5-*lm*]carbazol-7-one (**8a**).*

Method A. A stirred mixture of 2-phenyl-7*H*-[1,2,5]thiadiazolo[3,4-*b*][1,2,4]triazino[1,6,5-*mn*]-phenothiazin-7-one (**7a**) (38.7 mg, 0.1 mmol) and *m*-terphenyl (115.2 mg, 0.5 mmol) under an argon atmosphere was immersed into a preheated (~270 °C) Wood's metal bath for 3 h. After 3 h the thiazinone **7a** was fully consumed (by TLC) and the reaction was judged complete. The mixture was left to cool down to *ca*. 20 °C, diluted with DCM and poured onto a short silica pad, washed with DCM to remove remaining *m*-terphenyl and by-products and then chromatographed (DCM/*t*-BuOMe, 80:20) to afford the *title compound* **8a** (34.8 mg, 98%) as maroon needles; mp (hot-stage) not observed; mp (DSC) onset: 304.9 °C, peak max: 307.7 °C (*c*-hexane/PhMe, 90:10); R_f 0.43 (*n*-hexane/DCM/*t*-BuOMe, 60:30:10); R_f 0.87 (*n*-hexane/DCM/*t*-BuOMe, 30:60:10); Anal. Calcd for $C_{19}H_9N_5OS$: C, 64.22; H, 2.55; N, 19.71. Found: C, 64.49; H, 2.46; N, 20.04%; λ_{max}(DCM)/nm 247 (log ε 4.19), 273 (4.26), 299 (4.41), 317 (4.22), 378 (3.82), 392 (3.77), 413 (3.67), 466 inf (3.11),

496 (3.17), 530 (3.13), 572 inf (2.85); ν_{max}/cm^{-1} 1661s, 1649s, 1613m, 1530m, 1503m, 1493m, 1466s, 1449s, 1437m, 1343m, 1335m, 1263m, 1236m, 1161s, 1148m, 1115m, 1017m, 934m, 912m, 847m, 818s, 783m, 770m, 758m, 747s, 743s; δ_H(500 MHz, 50 °C, CD_2Cl_2) 8.68-8.67 (2H, m), 8.56 (1H, d, *J* 7.5), 8.48 (1H, d, *J* 8.0), 7.79 (1H, dd, *J* 7.5, 7.0), 7.74 (1H, dd, *J* 8.0, 7.5), 7.65-7.63 (3H, m); *m*/*z* (MALDI-TOF) 356 (MH^+, 100%), 355 (M^+, 11), 339 (34), 333 (37).

Method B. To a stirred solution of 2-phenyl-6*H*-[1,2,4]triazino[5,6,1-*jk*]carbazol-6-one (**9**) (59.5 mg, 0.2 mmol) in DMF (4.0 mL) at *ca.* 20 °C under an argon atmosphere, was added S_4N_4 (73.7 mg, 0.4 mmol) and the reaction mixture was then immersed into a preheated (~153 °C) Wood's metal bath. Additional S_4N_4 (4 × 73.7 mg) was added portion wise over a period of 5 h. After a total of 7 h heating, the reaction was allowed to cool to *ca.* 20 °C and extracted with 50:50 H_2O/DCM (100 mL). The organic layer was separated, washed with additional H_2O (20 mL), dried ($MgSO_4$), filtered and volatiles were removed *in vacuo*. Chromatography (DCM/*t*-BuOMe, 80:20) gave the *title compound* **8a** (56.1 mg, 79%) as maroon needles; mp (hot-stage) not observed; mp (DSC) onset: 304.9 °C, peak max: 307.7 °C (*c*-hexane/PhMe, 90:10); R_f 0.87 (*n*-hexane/DCM/*t*-BuOMe, 30:60:10); λ_{max}(DCM)/nm 247 (log ε 4.19), 273 (4.26), 299 (4.41), 317 (4.22), 378 (3.82), 392 (3.77), 413 (3.67), 466 inf (3.11), 496 (3.17), 530 (3.13), 572 inf (2.85); ν_{max}/cm^{-1} 1661s, 1649s, 1613m, 1530m, 1503m, 1493m, 1466s, 1449s, 1437m, 1343m, 1335m, 1321w, 1263m, 1236m, 1161s, 1148m, 1115m, 1017m, 934m, 912m, 847m, 818s, 783m, 770m, 758m, 747s, 743s; *m*/*z* (MALDI-TOF) 356 (MH^+, 100%), 355 (M^+, 11), 339 (34), 333 (37); identical to the one described above.

*4.8.2. 2-(Trifluoromethyl)-7*H*-[1,2,5]thiadiazolo[3,4-*b*][1,2,4]triazino[1,6,5-*lm*]carbazol-7-one (**8b**). Method A.* A stirred mixture of 2-(trifluoromethyl)-7*H*-[1,2,5]thiadiazolo[3,4-*b*][1,2,4]-triazino[1,6,5-*mn*]phenothiazin-7-one (**7b**) (37.9 mg, 0.1 mmol) and *m*-terphenyl (115.2 mg, 0.5 mmol) under an argon atmosphere was immersed into a preheated (~270 °C) Wood's metal bath for 3 h. After 3 h the thiazinone **7b** was fully consumed (by TLC) and the reaction was judged

complete. The mixture was left to cool down to *ca*. 20 °C, diluted with DCM and poured onto a short-pad of silica, which was washed with DCM to remove remaining *m*-terphenyl and minor by-products and then chromatographed (DCM/*t*-BuOMe, 80:20) to afford the *title compound* **8b** (33.7 mg, 97%) as maroon needles; mp (hot-stage) not observed; mp (DSC) onset: 274.7 °C, peak max: 277.9 °C (*c*-hexane/PhMe, 90:10); R_f 0.89 (*n*-hexane/DCM/*t*-BuOMe, 30:60:10); Anal. Calcd for $C_{14}H_4F_3N_5OS$: C, 48.42; H, 1.16; N, 20.17. found: C, 48.29; H, 1.44; N, 20.13%; λ_{max}(DCM)/nm 247 inf (log ε 4.38), 270 (4.55), 295 inf (4.32), 305 (4.39), 317 (4.38), 345 inf (3.81), 366 (4.01), 386 inf (3.97), 407 (4.00), 469 inf (3.24), 499 (3.33), 531 (3.29), 578 inf (2.97); ν_{max}/cm^{-1} 1659s, 1597m, 1530m, 1467m, 1413m, 1379s, 1352m, 1335m, 1306m, 1263m, 1246m, 1204s, 1144s, 1113s, 1103m, 1040s, 941s, 889m, 826s, 777s, 758s, 729s; δ_H(500 MHz, $CDCl_3$) 8.63 (1H, d, *J* 8.0), 8.44 (1H, d, *J* 8.5), 7.86 (1H, ddd, *J* 8.0, 8.0, 1.0), 7.79 (1H, dd, *J* 7.8, 7.8, 1.0); δ_C(125 MHz, $CDCl_3$) 170.0 (s, *C*=O), 161.1 (s), 153.6 (s), 149.2 (s), 148.0 (q, $^2J_{CF}$ 38.8), 134.7 (s), 130.5 (d), 128.3 (s), 128.0 (d), 126.1 (s), 123.7 (d), 119.4 (q, $^1J_{CF}$ 273.8), 113.5 (d), 108.1 (s); *m*/*z* (MALDI-TOF) 349 (MH^++1, 69%), 348 (MH^+, 100).

4.9. Synthesis of 1,2,5-Thiadiazolo-1,2,4-benzotriazin-7-ylidenemalononitriles 10a-b.

*4.9.1. 2-(6,8-Diphenyl[1,2,5]thiadiazolo[3',4':5,6]benzo[1,2-*e*][1,2,4]triazin-4(6*H*)-ylidene)-malononitrile (**10a**).* To a stirred solution of 6,8-diphenyl[1,2,5]thiadiazolo[3',4':5,6]benzo[1,2-*e*]-[1,2,4]triazin-4(6*H*)-one (**5a**) (71.5 mg, 0.2 mmol) in toluene (2 mL) at *ca.* 20 °C was added TCNEO (43.3 mg, 0.3 mmol) and the reaction mixture was then immersed into a pre-heated (~115 °C) oil bath. The reaction mixture was then heated at reflux for 1 h, cooled to *ca*. 20 °C, poured over a silica flash column and chromatographed (DCM) to afford the *title compound* **10b** (24.3 mg, 30%) as brown shiny needles; mp (hot-stage) not observed; mp (DSC) onset: 392.6 °C, peak max: 394.6 °C (PhMe), R_f 0.83 (DCM/*t*-BuOMe, 90:10); Anal. Calcd for $C_{22}H_{11}N_7S$: C, 65.17; H, 2.73; N, 24.18. Found: C, 64.99; H, 2.68; N, 24.15%; λ_{max}(DCM)/nm 279 (log ε 4.07), 311 (4.02), 320 (4.01), 352 inf (3.86), 403 (3.46), 477 inf (3.96), 503 (4.08), 583 inf (3.43), 631 (3.47), 687 inf

(3.40), 772 inf (3.04); ν_{max}/cm^{-1} 3067w (aryl C-H), 2205s and 2193m (C≡N), 1530s, 1526s, 1493s, 1460m, 1423m, 1385s, 1358m, 1281s, 1244m, 945m, 910w, 853m, 843m, 743m; δ_H(500 MHz, $CDCl_3$) 8.35 (2H, dd, *J* 8.0, 1.0), 7.73 (2H, dd, *J* 7.3, 7.3), 7.68–7.64 (3H, m), 7.56–7.51 (3H, m), 6.70 (1H, s, *H*-8); δ_C(125 MHz, DMSO-d_6) 153.9 (s), 152.4 (s), 150.9 (s), 150.5 (s), 145.0 (s), 140.8 (s), 138.5 (s), 132.7 (s), 131.5 (d), 131.1 (d), 130.5 (d), 129.2 (d), 126.7 (d), 125.6 (d), 116.6 (s, *C*≡N), 116.5 (s, *C*≡N), 93.9 (d), 58.2 [s, *C*$(CN)_2$]; *m/z* (MALDI-TOF, DHB matrix) 407 (MH^++1, 21%), 406 (MH^+, 100), 405 (M^+, 56).

*4.9.2. 2-[6-Phenyl-8-(trifluoromethyl)[1,2,5]thiadiazolo[3',4':5,6]benzo[1,2-*e*][1,2,4]triazin-4(6*H*)-ylidene]malononitrile* (**10b**). To a stirred solution of 6-phenyl-8-(trifluoromethyl)[1,2,5]thiadiazolo-[3',4':5,6]benzo[1,2-*e*][1,2,4]triazin-4(6*H*)-one (**5b**) (69.9 mg, 0.2 mmol) in toluene (2 mL) at *ca.* 20 °C was added TCNEO (43.3 mg, 0.3 mmol) and then the reaction mixture was immersed into a pre-heated (~115 °C) oil bath. The reaction mixture was heated at reflux for 1 h, cooled to *ca*. 20 °C, poured over a silica flash column and chromatographed (DCM) to afford the *title compound* **10b** (20.7 mg, 26%) as green plates; mp (hot-stage) sublimation 279.1–285.3 °C; mp (DSC) onset: 288.2 °C, peak max: 288.5 °C (PhMe), R_f 0.88 (DCM/*t*-BuOMe; 90:10); Anal. Calcd for $C_{17}H_6F_3N_7S$: C, 51.39; H, 1.52; N, 24.68. Found: C, 51.28; H, 1.48; N, 24.57%; λ_{max}(DCM)/nm 271 inf (log ε 3.69), 298 (3.84), 369 (3.35), 390 (3.32), 446 (3.68), 473 (3.80), 524 inf (1.98), 573 (3.11), 623 (3.17), 679 (3.09), 762 inf (2.72); ν_{max}/cm^{-1} 3044w (aryl C-H), 2214s (C≡N), 1545s, 1508m, 1491m, 1420s, 1371s, 1277s, 1263m, 1221m, 1198s, 1179m, 1157m, 1148s, 1117s, 1065s, 949m, 858s, 845m, 829m, 799m, 772m, 739s; δ_H(500 MHz, $CDCl_3$) 7.73–7.65 (3H, m), 7.58-7.56 (2H, m), 6.70 (1H, s, *H*-8); δ_C(125 MHz, $CDCl_3$) 154.3 (s), 152.7 (s), 149.8 (s), 144.9 (s), 144.7 (q, $^2J_{CF}$ 39.6), 139.6 (s), 136.4 (s), 131.8 (d), 131.0 (d), 124.7 (d), 118.7 (q, $^1J_{CF}$ 272.9), 114.5 (s, *C*≡N), 114.2 (s, *C*≡N), 96.4 (d), 70.9 [s, *C*$(CN)_2$]; *m/z* (MALDI-TOF) 399 (MH^++1, 20%), 398 (MH^+, 57), 397 (M^+, 100), 153 (57).

ASSOCIATED CONTENT

Supporting Information Available.

Crystallographic, computational, UV-vis, CV, NMR, DSC and TGA data and discussion (PDF). Crystallographic file for compounds **2b**, **2d**, **4c** and **10b** (CIF). This material is available free of charge *via* the Internet at http://pubs.acs.org.

AUTHOR INFORMATION

Corresponding Author

*E-mail: Koutenti@ucy.ac.cy

Notes

The authors declare no competing financial interest.

ACKNOWLEDGMENTS

The authors thank the University of Cyprus and the Cyprus Research Promotion Foundation.

REFERENCES

(1) Liu, Y.; Li, J.; Tschirhart, T.; Terrell, J. L.; Kim, E.; Tsao, C-Y.; Kelly, D. L.; Bentley, W. E.; Payne, G. F. Connecting Biology to Electronics: Molecular Communication via Redox Modality. *Adv. Healthcare Mater.* **2017**, *6*, 1700789.

(2) (a) Wikström, M.; Sharma, V.; Kaila, V. R. I.; Hosler, J. P.; Hummer, G. New Perspectives on Proton Pumping in Cellular Respiration. *Chem. Rev*. **2015**, *115*, 2196-2221. (b) Blumberger, J. Recent Advances in the Theory and Molecular Simulation of Biological Electron Transfer Reactions. *Chem. Rev*. **2015**, *115*, 11191-11238. (c) Jones, D. P.; Sies, H. The Redox Code. *Antioxid. Redox Signal.* **2015**, *23*, 734-746. (d) Circu, M. L.; Aw, Y. T. Reactive Oxygen Species, Cellular Redox Systems, and Apoptosis. *Free Radical Biol. Med.* **2010**, *48*, 749–762. (e) Kang, J.;

Pervaiz, S. Mitochondria: Redox Metabolism and Dysfunction. *Biochem. Res. Int.* **2012**, *2012*, 896751.

(3) (a) Noctor, G.; Reichheld, J.-P.; Foyer, C. H. ROS-Related Redox Regulation and Signaling in Plants. *Semin. Cell Dev. Biol.* **2018**, *80*, 3-12. (b) Pfannschmidt, T. Chloroplast Redox Signals: How Photosynthesis Controls its Own Genes. *Trends Plant Sci.* **2003**, *8*, 33-41.

(4) (a) Xiao, W.; Wang, D. The Electrochemical Reduction Processes of Solid Compounds in High Temperature Molten Salts. *Chem. Soc. Rev*. **2014**, *43*, 3215-3228. (b) Dominguez-Benetton, X.; Varia, J. C.; Pozo, G.; Modin, O.; Heijne, A. T.; Fransaer, J.; Rabaey, K. Metal Recovery by Microbial Electro-Metallurgy. *Progr. Mat. Sci.* **2018**, *94*, 435-461. (c) Tang, Y.; Xu, S.; Dai, Y.; Yan, X.; Li, R.; Xiao, L.; Fan, J. Solid Phase Metallurgy Strategy to Sub-5 Nm Au–Pd and Ni–Pd Bimetallic Nanoparticles with Controlled Redox Properties. *Chem. Commun*. **2014**, *50*, 213-215.

(5) (a) Li, S.; Zhao, C.; Wang, Y.; Li, H.; Li, Y. Synthesis and Electrochemical Properties of Electroactive Aniline-Dimer-Based Benzoxazines for Advanced Corrosion-Resistant Coatings. *J. Mat. Sci*. **2018**, *53*, 7344-7356. (b) Cai, W.; Wang, J.; Quan, X.; Zhao, S.; Wang, Z. Antifouling and Anticorrosion Properties of One-Pot Synthesized Dedoped Bromo-Substituted Polyaniline and its Composite Coatings. *Surf. Coat. Techn.* **2018**, *334*, 7-18. (c) Yang, C.; Wei, H.; Guan, L.; Guo, J.; Wang, Y.; Yan, X.; Zhang, X.; Wei, S.; Guo, Z. Polymer Nanocomposites for Energy Storage, Energy Saving, and Anticorrosion. *J. Mater. Chem. A* **2015**, *3*, 14929-14941. (d) Adriaens, A.; Dowsett, M. The Coordinated Use of Synchrotron Spectroelectrochemistry for Corrosion Studies on Heritage Metals. *Acc. Chem. Res.* **2010**, *43*, 927-935. (e) Spinks, G. M.; Dominis, A. J.; Wallace, G. G.; Tallman, D. E. Electroactive Conducting Polymers for Corrosion Control. Part 2. Ferrous Metals. *J. Solid State Electrochem.* **2002**, *6*, 85-100. (f) Tallman, D. E.; Spinks, G. M.; Dominis, A.; Wallace, G. G. Electroactive Conducting Polymers for Corrosion Control. Part 1. General Introduction and a Review of Non-Ferrous Metals. *J. Solid State Electrochem.* **2002**, *6*, 73-85.

(6) (a) Nimse, S. B.; Pal, D. Free Radicals, Natural Antioxidants, and Their Reaction Mechanisms. *RSC Adv*. **2015**, *5*, 27986-28006. (b) Pisoschi, A. M.; Cimpeanu, C.; Predoi, G. Electrochemical Methods for Total Antioxidant Capacity and its Main Contributors Determination: A Review. *Open Chem.* **2015**, *13*, 824-856. (c) Batinic-Haberle, I.; Spasojevic, I. Complex Chemistry and Biology of Redox-Active Compounds, Commonly Known as SOD Mimics, Affect Their Therapeutic Effects. *Antioxid. Redox Signaling.* **2014**, *20*, 2323-2325. (d) Halvorsen, B. L.; Carlsen, M. H.; Phillips, K. M.; Bøhn, S. K.; Holte, K.; Jacobs Jr., D. R.; Blomhoff, R. Content of Redox-Active Compounds (ie, Antioxidants) in Foods Consumed in the United States. *Am. J. Clin. Nutr.* **2006**, *84*, 95-135.

(7) (a) Gsänger, M.; Bialas, D.; Huang, L.; Stolte, M.; Würthner, F. Organic Semiconductors Based on Dyes and Color Pigments. *Adv. Mater.* **2016**, *28*, 3615-3645. (b) Mayer, M. T.; Lin, Y.; Yuan, G.; Wang, D. Forming Heterojunctions at the Nanoscale for Improved Photoelectrochemical Water Splitting by Semiconductor Materials: Case Studies on Hematite. *Acc. Chem. Res.* **2013**, *46*, 1558-1566.

(8) (a) Barsan, M. M.; Ghica, M. E.; Brett, C. M. A. Electrochemical Sensors and Biosensors Based on Redox Polymer/Carbon Nanotube Modified Electrodes: A Review. *Anal. Chim. Acta*. **2015**, *881*, 1-23. (b) Wang, J.; Musameh, M. A Reagentless Amperometric Alcohol Biosensor Based on Carbon-Nanotube/Teflon Composite Electrodes. *Anal. Lett.* **2003**, *36*, 2041-2048.

(9) (a) Li, J.; Wu, N. Semiconductor-Based Photocatalysts and Photoelectrochemical Cells for Solar Fuel Generation: A Review. *Catal. Sci. Technol*. **2015**, *5*, 1360-1384. (b) Milshtein, J. D.; Barton, J. L.; Darling, R. M.; Brushett, F. R. 4-Acetamido-2,2,6,6-tetramethylpiperidine-1-oxyl as a Model Organic Redox Active Compound for Nonaqueous Flow Batteries. *J. Power Sources.* **2016**, *327*, 151-159. (c) Xiang, Y.; Lu, S.; Jiang, S. P. Layer-by-Layer Self-Assembly in the Development of Electrochemical Energy Conversion and Storage Devices from Fuel Cells to Supercapacitors. *Chem. Soc. Rev*. **2012**, *41*, 7291-7321.

(10) Ballard, N.; Mecerreyes, D.; Asua, J. M. Redox Active Compounds in Controlled Radical Polymerization and Dye-Sensitized Solar Cells: Mutual Solutions to Disparate Problems. *Chem. – Eur. J.* **2015**, *21*, 18516-18527.

(11) Arias, Z. G.; Álvarez, J. L. M.; Fonseca, J. M. L. Electrochemical Characterization of the Self□Assembled Monolayer of 6□Thioguanine on the Mercury Electrode. *Electroanalysis* **2004**, *16*, 1044-1050.

(12) (a) Zieleniewska, A.; Lodermeyer, F.; Roth, A.; Guldi, D. M. Fullerenes-How 25 Years of Charge Transfer Chemistry Have Shaped our Understanding of (Interfacial) Interactions. *Chem. Soc. Rev.* **2018**, *47*, 702-714. (b) Stace, A. J.; O'Brien, P. Fullerenes: Past, Present and Future, Celebrating the 30th Anniversary of Buckminster Fullerene. *Philos. Trans. R. Soc., A* **2016**, *374*, 20160278.

(13) (a) Martín, N.; Segura, J. L.; Seoane, C. Design and Synthesis of TCNQ and DCNQI Type Electron Acceptor Molecules as Precursors for 'Organic metals'. *J. Mater. Chem.* **1997**, *7*, 1661-1676. (b) Schein, L. B.; Nigrey, P. J. Electron Mobilities in Tetracyanoquinodimethane. *Phys. Rev. B* **1978**, *18*, 2929-2930.

(14) (a) Eynde, J. J. V.; Delfosse, F.; Mayence, A.; Haverbeke, Y. V. Old Reagents, New Results: Aromatization of Hantzsch 1,4-Dihydropyridines with Manganese Dioxide and 2,3-Dichloro-5,6-dicyano-1,4-benzoquinone. *Tetrahedron* **1995**, *51*, 6511-6516. (b) Liu, L.; Floreancig, P. E. 2,3-Dichloro-5,6-dicyano-1,4-benzoquinone-Catalyzed Reactions Employing MnO_2 as a Stoichiometric Oxidant. *Org. Lett.* **2010**, *12*, 4686-4689. (c) Bharate, S. B. 2,3-Dichloro-5,6-dicyano-1,4-benzoquinone (DDQ). *Synlett* **2006**, 496-497.

(15) (a) Martín, N. Tetrathiafulvalene: The Advent of Organic Metals. *Chem. Commun.* **2013**, *49*, 7025-7027. (b) Jana, A.; Ishida, M.; Park, J. S.; Bähring, S.; Jeppesen, J. O.; Sessler, J. L. Tetrathiafulvalene- (TTF-) Derived Oligopyrrolic Macrocycles. *Chem. Rev.* **2017**, *117*, 2641-2710.

(16) (a) Astruc, D. Why is Ferrocene so Exceptional? *Eur. J. Inorg. Chem.* **2017**, *2017*, 6-29. (b) Werner, H. At Least 60 Years of Ferrocene: The Discovery and Rediscovery of the Sandwich Complexes. *Angew. Chem., Int. Ed.* **2012**, *51*, 6052-6058.

(17) (a) Zhou, Z.; Liu, L. TEMPO and its Derivatives: Synthesis and Applications. *Curr. Org. Chem.* **2014**, *18*, 459-474. (b) Megiel, E. Surface Modification Using TEMPO and its Derivatives. *Adv. Colloid Interface Sci.* **2017**, *250*, 158-184.

(18) Mazzio, K. A.; Luscombe, C. K. The Future of Organic Photovoltaics. *Chem. Soc. Rev.* **2015**, *44*, 78-90.

(19) (a) Er, S.; Suh, C.; Marshak, M. P.; Aspuru-Guzik, A. Computational Design of Molecules for an All-Quinone Redox Flow Battery. *Chem. Sci.* **2015**, *6*, 885-893. (b) Huskinson, B.; Marshak, M. P.; Suh, C.; Er, S.; Gerhardt, M. R.; Galvin, C. J.; Chen, X.; Aspuru-Guzik, A.; Gordon, R. G.; Aziz, M. J. A Metal-Free Organic-Inorganic Aqueous Flow Battery. *Nature* **2014**, *505*, 195-198.

(20) Zotti, G.; Zecchin, S.; Vercelli, B.; Berlin, A.; Casado, J.; Hernández, V.; Ortiz, R. P.; López Navarrete, J. T.; Ortí, E.; Viruela, P. M.; Milián, B. Magnetic and Conductive Properties of Quinoidal Oligothiophenes. *Chem. Mater.* **2006**, *18*, 1539-1545.

(21) (a) Zissimou, G. A.; Kourtellaris, A.; Koutentis, P. A. Oxidation of Isodiphenylfluorindine: Routes to 13-Oxoisodiphenylfluorindinium Perchlorate and Fluorindine Cruciform Dimers. *Org. Lett.* **2018**, *20*, 844-847. (b) Kalogirou, A. S.; Kourtellaris, A.; Koutentis, P. A. The Acid and/or Thermal Mediated Ring Contraction of 4*H*-1,2,6-Thiadiazines to Afford 1,2,5-Thiadiazoles. *Org. Lett.* **2016**, *18*, 4056-4059. (c) Koyioni, M.; Manoli, M.; Koutentis, P. A. The Reaction of DABCO with 4-Chloro-5*H*-1,2,3-dithiazoles: Synthesis and Chemistry of 4-[*N*-(2-Chloroethyl)piperazin-1-yl]-5*H*-1,2,3-dithiazoles. *J. Org. Chem.* **2016**, *81*, 615-631.

(22) Blatter, H. M.; Lukaszewski, H. A New Stable Free Radical. *Tetrahedron Lett.* **1968**, *9*, 2701-2705.

(23) (a) Savva, A. C.; Mirallai, S. I.; Zissimou, G. A.; Berezin, A. A.; Demetriades, M.; Kourtellaris, A.; Constantinides, C. P.; Nicolaides, C.; Trypiniotis, T.; Koutentis, P. A. Preparation of Blatter Radicals via Aza-Wittig Chemistry: The Reaction of *N*-Aryliminophosphoranes with 1-(Het)aroyl-2-aryldiazenes. *J. Org. Chem.* **2017**, *82*, 7564-7575. (b) Berezin, A. A.; Zissimou, G.; Constantinides, C. P.; Beldjoudi, Y.; Rawson, J. M.; Koutentis, P. A. Route to Benzo- and Pyrido-fused 1,2,4-Triazinyl Radicals via *N*′-(Het)aryl-*N*′-[2-nitro(het)aryl]hydrazides. *J. Org. Chem.* **2014**, *79*, 314-327. (c) Koutentis, P. A.; Lo Re, D. Catalytic Oxidation of *N*-Phenylamidrazones to 1,3-Diphenyl-1,4-dihydro-1,2,4-benzotriazin-4-yls: An Improved Synthesis of Blatter's Radical. *Synthesis* **2010**, 2075-2079.

(24) Neugebauer, F. A.; Umminger, I. Über 1,4□Dihydro□1,2,4□benzotriazinyl□Radikale. *Chem. Ber.* **1980**, *113*, 1205-1225.

(25) Constantinides, C. P.; Koutentis, P. A.; Krassos, H.; Rawson, J. M.; Tasiopoulos, A. J. Characterization and Magnetic Properties of a "Super Stable" Radical 1,3-Diphenyl-7-trifluoromethyl-1,4-dihydro-1,2,4-benzotriazin-4-yl. *J. Org. Chem.* **2011**, *76*, 2798-2806.

(26) (a) Koutentis, P. A.; Krassos, H.; Lo Re, D. 1,3-Diphenylbenzo[*e*][1,2,4]triazin-7(1*H*)-one: Selected Chemistry at the C-6, C-7 and C-8 Positions. *Org. Biomol. Chem.* **2011**, *9*, 5228-5237. (b) Koutentis, P. A.; Loizou, G.; Lo Re, D. Synthesis of Triazafluoranthenones via Silver(I)-Mediated Nonoxidative and Oxidative Intramolecular Palladium-Catalyzed Cyclizations. *J. Org. Chem.* **2011**, *76*, 5793-5802.

(27) Berezin, A. A.; Constantinides, C. P.; Mirallai, S. I.; Manoli, M.; Cao, L. L.; Rawson, J. M.; Koutentis, P. A. Synthesis and Properties of Imidazolo-Fused Benzotriazinyl Radicals. *Org. Biomol. Chem.* **2013**, *11*, 6780-6795.

(28) Ioannou, T. A.; Koutentis, P. A.; Krassos, H.; Loizou, G.; Lo Re, D. Some Cyclization Reactions of 1,3-Diphenylbenzo[*e*][1,2,4]triazin-7(1*H*)-one: Preparation and Computational Analysis of Non Symmetrical Zwitterionic Biscyanines. *Org. Biomol. Chem.* **2012**, *10*, 1339-1348.

(29) Monks, T. J.; Jones, D. C. The Metabolism and Toxicity of Quinones, Quinonimines, Quinone Methides, and Quinone-Thioethers. *Curr. Drug Metab.* **2002**, *3*, 425-438.

(30) (a) Keane, L.-A. J.; Mirallai, S. I.; Sweeney, M.; Carty, M. P.; Zissimou, G. A.; Berezin, A. A.; Koutentis, P. A.; Aldabbagh, F. Anti-Cancer Activity of Phenyl and Pyrid-2-yl 1,3-Substituted Benzo[1,2,4]triazin-7-ones and Stable Free Radical Precursors. *Molecules* **2018**, *23*, 574. (b) Sweeney, M.; Coyle, R.; Kavanagh, P.; Berezin, A. A.; Lo Re, D.; Zissimou, G. A.; Koutentis, P. A.; Carty, M. P.; Aldabbagh, F. Discovery of Anti-Cancer Activity for Benzo[1,2,4]triazin-7-ones: Very Strong Correlation to Pleurotin and Thioredoxin Reductase Inhibition. *Bioorg. Med. Chem.* **2016**, 24, 3565-3570.

(31) Catto, M.; Berezin, A. A.; Lo Re, D.; Loizou, G.; Demetriades, M.; De Stradis, A.; Campagna, F.; Koutentis, P. A.; Carotti, A. Design, Synthesis and Biological Evaluation of Benzo[*e*][1,2,4]triazin-7(1*H*)-one and [1,2,4]-Triazino[5,6,1-*jk*]carbazol-6-one Derivatives as Dual Inhibitors of *β*-Amyloid Aggregation and Acetyl/Butyryl Cholinesterase. *Eur. J. Med. Chem.* **2012**, *58*, 84-97.

(32) Lonchakov, A. V.; Rakitin, O. A.; Gritsan, N. P.; Zibarev, A. V. Breathing Some New Life into an Old Topic: Chalcogen-Nitrogen π-Heterocycles as Electron Acceptors. *Molecules* **2013**, *18*, 9850-9900.

(33) Hansch, C.; Leo, A.; Taft, R. W. A Survey of Hammett Substituent Constants and Resonance and Field Parameters. *Chem. Rev.* **1991**, *91*, 165-195.

(34) (a) Mukai, K.; Inoue, K.; Achiwa, N.; Jamali, J. B.; Krieger, C.; Neugebauer, F. A. Magnetic-Properties of 1,4-Dihydro-1,2,4-benzotriazin-4-yl Radicals. *Chem. Phys. Lett.* **1994**, *224*, 569-575.

(b) Kadirov, M. K.; Buzykin, B. I.; Gazetdinova, N. G. Electron Spin and Electron Nuclear Double Resonances of the Stable 1-(4-Nitrophenyl)-3-phenyl-1,4-dihydro-1,2,4-benzotriazin-4-yl Free Radical. *Russ. Chem. Bull.* **2002**, *51*, 1796-1799. (c) Gubaidullin, A. T.; Buzykin, B. I.; Litvinov, I. A.; Gazetdinova, N. G. Molecular and Crystal Structure of a Superstable Free Radical, 1,3-Diphenyl-1,4-dihydro-1,2,4-benzotriazin-4-yl. *Russ. J. Gen. Chem.* **2004**, *74*, 939-943. (d) Miura, Y.; Yoshioka, N. π-Stacked Structure of Thiadiazolo-Fused Benzotriazinyl Radical: Crystal Structure and Magnetic Properties. *Chem*. *Phys*. *Lett.* **2015**, *626*, 11-14.

(35) Freeman, F. Properties and Reactions of Ylidenemalononitriles. *Chem. Rev.* **1980**, *80*, 329-350.

(36) Koutentis, P. A.; Rees, C. W. Reaction of Herz Salts with Malononitrile: a General Route to (6*H*-Benzo[1,2,3]dithiazol-6-ylidene)malononitriles. *J. Chem. Soc.*, *Perkin Trans. 1* **2002**, 315-319.

(37) (a) Du, J.; Biewer, M. C.; Stefan, M. C. Benzothiadiazole Building Units in Solution-Processable Small Molecules for Organic Photovoltaics. *J. Mater. Chem. A* **2016**, *4*, 15771-15787. (b) Wang, Y.; Michinobu, T. Benzothiadiazole and its π-Extended, Heteroannulated Derivatives: Useful Acceptor Building Blocks for High-performance Donor-acceptor Polymers in Organic Electronics. *J. Mater. Chem. C* **2016**, *4*, 6200-6214. (c) Parker, T. C.; Patel, D. G.; Moudgil, K.; Barlow, S.; Risko, C.; Brédas, J.-L.; Reynolds, J. R.; Marder, S. R. Heteroannulated Acceptors Based on Benzothiadiazole. *Mater. Horiz.* **2015**, *2*, 22-36.

(38) (a) Koutentis, P. A. *Comprehensive Heterocyclic Chemistry III*; Zhdankin, V. V., Ed.; Katritzky, A. R., Ramsden, C. A., Scriven, E. F. V., Taylor, R. J. K., Eds; Elsevier: Oxford, U.K., **2008**; Vol. 5, Chapter 5.09, pp 515−565. (c) Todres, Z. V. *Chalcogenadiazoles: Chemistry and Applications*; CRC Press, Taylor & Francis Group: Boca Raton, FL, **2012**; Chapter 2, pp 153−181. (d) Konstantinova, L. S.; Knyazeva, E. A.; Rakitin, O. A. Recent Developments in the Synthesis and Applications of 1,2,5-Thia- and Selenadiazoles. A Review. *Org. Prep. Proced. Int.* **2014**, *46*, 475−544.

(39) Shi, S.; Katz, T. J.; Yang, B. V.; Liu, L. Use of Thiazyl Chlorides, Alkyl Carbamates, and Thionyl Chloride to Fuse 1,2,5-Thiadiazoles to Quinones and to Oxidize, Chlorinate, and Aminate Them. *J. Org. Chem.* **1995**, *60*, 1285-1297.

(40) Marcos, C. F.; Polo, C.; Rakitin, O. A.; Rees, C. W.; Torroba, T. One-Pot Synthesis and Chemistry of Bis[1,2]dithiolopyrroles. *Chem. Commun.* **1997**, 879-880.

(50) Bond lengths in crystalline organic compounds. *CRC Handbook of Chemistry and Physics*; Lide, D. R., Ed, 75th Edition; CRC Press, Inc.: Boca Raton, Florida, **1994**.

(51) Singh, S. P.; Kumar, C. P.; Sharma, G. D.; Kurchania, R.; Roy, M. S. Synthesis of a Modified PC70BM and Its Application as an Electron Acceptor with Poly(3-hexylthiophene) as an Electron Donor for Efficient Bulk Heterojunction Solar Cells. *Adv. Funct. Mater*. **2012**, *2*, 4087-4095.

(52) Ahmed, E.; Ren, G.; Kim, F. S.; Hollenbeck, E. C; Jenekhe, S. A. Design of New Electron Acceptor Materials for Organic Photovoltaics: Synthesis, Electron Transport, Photophysics, and Photovoltaic Properties of Oligothiophene-Functionalized Naphthalene Diimides. *Chem. Mater*. **2011**, *23*, 4563–4577.

(53) Harwood, L. M. "Dry-Column" Flash Chromatography. *Aldrichimica Acta* **1985**, *18*, 25-25.

(54) Cohen, L. H.; Gusev, A. I. Small Molecule Analysis by MALDI Mass Spectrometry. *Anal. Bioanal. Chem.* **2002**, *373*, 571-586.

(55) Langley, G. J.; Herniman, J. M.; Townell M. S. 2B or not 2B, that is the Question: Further Investigations into the Use of Pencil as a Matrix for Matrix□Assisted Laser Desorption/Ionisation. *Rapid Commun. Mass Spectrom*. **2007**, *21*, 180-190.

(56) (a) Becke-Goehring, M.; Jolly, W. L.; De La Camp, U.; Macomber, J. D.; Woeller, H. F. Sulfur Nitrides. *Inorganic Syntheses*; Rochow, E. G. Ed.; McGraw-Hill: New York, **1960**; Vol. 6; Ch. VIA, 123-125. (b) Villena-Blanco1, M.; Jolly, W. L.; Egan, B. Z.; Zingaro, R. A. Tetrasulfur

Tetranitride, S_4N_4. *Inorganic Syntheses*; Tyree, S. Y. Jr. Ed.; McGraw-Hill: New York, **1967**; Vol. 9; Ch. VI, 98-102.

(57) Linn, W. J. Tetracyanoethylene Oxide. *Org. Synth*. **1969**, *49*, 103-103.

(58) *CrysAlis CCD and CrysAlis RED*, version 1.171.32.15; Oxford Diffraction Ltd, Abingdon, Oxford, England, **2008**.

(59) (a) Sheldrick, G. M. Crystal Structure Refinement with *SHELXL*. *Acta Crystallogr. C Struct. Chem.* **2015**, *71*, 3-8. (b) Sheldrick, G. M. *SHELXL97*-A program for the refinement of crystal structure. University of Göttingen, Germany.

(60) Farrugia, L. J. *WinGX* Suite for Single Crystal Small Molecule Crystallography. *J. Appl. Crystallogr.* **1999**, *32*, 837-838.

(61) Brandenburg, K. DIAMOND, version 3.1d; Crystal Impact GbR, Bonn, Germany, **2006**.

(62) (a) Becke, A. D. Density□Functional Thermochemistry. III. The Role of Exact Exchange. *J. Chem. Phys.* **1993**, *98*, 5648-5652. (b) Lee, C. T.; Yang, W. T.; Parr, R. G. Development of the Colle-Salvetti Correlation-Energy Formula into a Functional of the Electron Density. *Phys. Rev. B* **1988**, *37*, 785-789.

(63) Scott, A. P.; Radom, L. Harmonic Vibrational Frequencies: An Evaluation of Hartree−Fock, Møller−Plesset, Quadratic Configuration Interaction, Density Functional Theory, and Semiempirical Scale Factors. *J. Phys. Chem.* **1996**, *100*, 16502-16513.

(64) Gaussian 03, Revision C.02, Frisch, M. J.; Trucks, G. W.; Schlegel, H. B.; Scuseria, G. E.; Robb, M. A.; Cheeseman, J. R.; Montgomery, Jr., J. A.; Vreven, T.; Kudin, K. N.; Burant, J. C.; Millam, J. M.; Iyengar, S. S.; Tomasi, J.; Barone, V.; Mennucci, B.; Cossi, M.; Scalmani, G.; Rega, N.; Petersson, G. A.; Nakatsuji, H.; Hada, M.; Ehara, M.; Toyota, K.; Fukuda, R.; Hasegawa, J.; Ishida, M.; Nakajima, T.; Honda, Y.; Kitao, O.; Nakai, H.; Klene, M.; Li, X.; Knox, J. E.;

Hratchian, H. P.; Cross, J. B.; Bakken, V.; Adamo, C.; Jaramillo, J.; Gomperts, R.; Stratmann, R. E.; Yazyev, O.; Austin, A. J.; Cammi, R.; Pomelli, C.; Ochterski, J. W.; Ayala, P. Y.; Morokuma, K.; Voth, G. A.; Salvador, P.; Dannenberg, J. J.; Zakrzewski, V. G.; Dapprich, S.; Daniels, A. D.; Strain, M. C.; Farkas, O.; Malick, D. K.; Rabuck, A. D.; Raghavachari, K.; Foresman, J. B.; Ortiz, J. V.; Cui, Q.; Baboul, A. G.; Clifford, S.; Cioslowski, J.; Stefanov, B. B.; Liu, G.; Liashenko, A.; Piskorz, P.; Komaromi, I.; Martin, R. L.; Fox, D. J.; Keith, T.; Al-Laham, M. A.; Peng, C. Y.; Nanayakkara, A.; Challacombe, M.; Gill, P. M. W.; Johnson, B.; Chen, W.; Wong, M. W.; Gonzalez, C.; Pople, J. A. Gaussian, Inc., Wallingford CT, **2004**.